

AD-A172 853

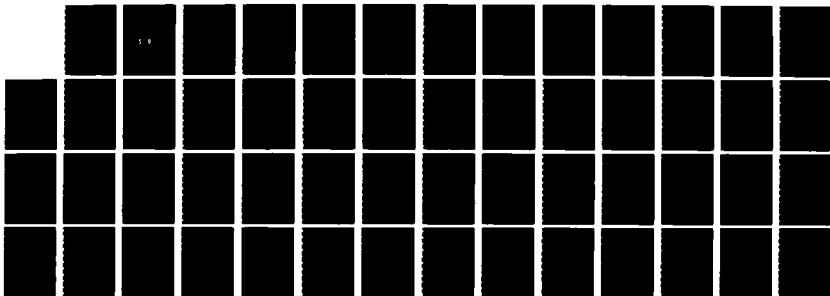
PSEUDOSPECTRAL METHOD FOR TRANSONIC FLOWS AROUND AN
AIRFOIL(U) FLOW INDUSTRIES INC KENT WA RESEARCH AND
TECHNOLOGY DIV W H JOU ET AL MAR 85 AFOSR-TR-86-0865
F49620-84-C-0027

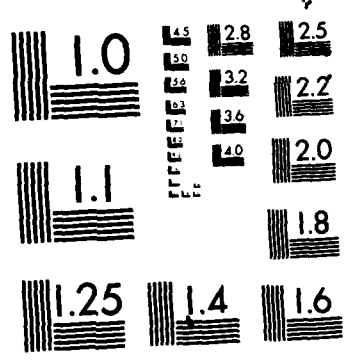
1/1

UNCLASSIFIED

F/G 20/4

NL





MICROCOPY RESOLUTION TEST CHART
NATIONAL BUREAU OF STANDARDS-1963-A

AD-A172 853

PSEUDOSPECTRAL METHOD FOR TRANSONIC FLOWS AROUND AN AIRFOIL

AIR FORCE OFFICE OF SCIENTIFIC RESEARCH (AFSC)
OFFICE OF TRANSMITTAL TO DTIC
This technical report has been reviewed and is
approved for public release IAW AFR 190-12.
Distribution is unlimited.

by MATTHEW J. KEMPER
Chief, Technical Information Division

W.-H. Jou and A. C. Mueller

DTIC
S ELECTE D
OCT 08 1985
D

Approved for public release;
distribution unlimited.

March 1985

DTIC FILE COPY



Flow Industries, Inc.
Research and Technology Division
21414 68th Avenue South
Kent, Washington 98032
(206) 872-8500
TWX: 910-447-2762

Approved for public release,
distribution unlimited

6c. ADDRESS (City, State and ZIP Code) RESEARCH AND TECHNOLOGY DIVISION 21414 68th AVENUE SOUTH KENT, WASHINGTON 98032			7b. ADDRESS (City, State and ZIP Code) BOLLING AFB DC 20332-6448		
8a. NAME OF FUNDING/SPONSORING ORGANIZATION AIR FORCE OFFICE OF SCIENTIFIC RESEARCH		8b. OFFICE SYMBOL (If applicable) NA	9. PROCUREMENT INSTRUMENT IDENTIFICATION NUMBER F49620-84-C-0027		
8c. ADDRESS (City, State and ZIP Code) BOLLING AFB DC 20332-6448			10. SOURCE OF FUNDING NOS.		
			PROGRAM ELEMENT NO. 61102F	PROJECT NO. 2307	TASK NO. A1
11. TITLE (Include Security Classification) PSEUDOSPECTRAL METHOD FOR TRANSONIC FLOWS AROUND AN AIRFOIL (UNCLASSIFIED)					
12. PERSONAL AUTHOR(S) Jou, W-H Mueller, A C					
13a. TYPE OF REPORT ANNUAL		13b. TIME COVERED FROM Feb 84 TO 31 Jan 85		14. DATE OF REPORT (Yr., Mo., Day) March 1985	
15. PAGE COUNT 49					
16. SUPPLEMENTARY NOTATION 7 This investigation					
17. COSATI CODES			18. SUBJECT TERMS (Continue on reverse if necessary and identify by block number)		
FIELD	GROUP	SUB. GR.	TRANSONIC FLOW, SPECTRAL METHOD, AIRFOIL		
19. ABSTRACT (Continue on reverse if necessary and identify by block number) The present investigation has attempted to construct a pseudospectral scheme that is highly accurate and competitive in computational efficiency with existing finite difference or finite volume methods. A hybrid scheme using spectral decomposition in the direction along the airfoil surface and a finite difference scheme in the other direction was found to be capable of resolving shock waves in one grid. Several filters have been studied. A low-pass filter in the spectral space was not able to stabilize the computation without seriously affecting the shock resolution. An algebraic filter that averages the flow variables around a grid point was capable of stabilizing the computations and maintaining the sharpness of the shock wave. The residue of the scheme did not decrease with time. The number of supersonic points in the flow field was taken as an indicator of convergence. Attempts to find another form of error norm were not successful. An explicit full spectral scheme studied with a Chebyshev polynomial expansion required excessive computing time and would not be competitive with a finite volume calculation using a dense grid. A					
20. DISTRIBUTION/AVAILABILITY OF ABSTRACT UNCLASSIFIED/UNLIMITED <input checked="" type="checkbox"/> SAME AS RPT. <input type="checkbox"/> DTIC USERS <input type="checkbox"/>			21. ABSTRACT SECURITY CLASSIFICATION Unclassified		

Flow Technical Report No. 325

PSEUDOSPECTRAL METHOD FOR
TRANSONIC FLOWS AROUND AN AIRFOIL*

by

W.-H. Jou and A. C. Mueller

March 1985

Flow Industries, Inc.
Research and Technology Division
21414 68th Avenue South
Kent, Washington 98032

*This work is supported by the Office of Naval Research and the Air Force
Office of Scientific Research under Contract No. F49620-84-C-0027.

Table of Contents

	Page
List of Figures	iii
List of Tables	iv
1. Introduction	1
2. Governing Equations and Basic Approach	3
3. Hybrid Scheme	5
3.1 Spatial and Temporal Discretizations	5
3.2 Boundary Conditions	6
3.3 Convergence Acceleration	7
3.4 Filter and Artificial Viscosity	9
3.5 Computed Results	11
4. Development of Full Spectral Method	15
4.1 Fourier Chebyshev Method	15
4.2 Polynomial Subtraction Method	17
5. Implicit Pseudospectral Method	19
5.1 Richardson Iteration	21
5.2 Convergence of Richardson Iteration	22
5.3 Finite Iteration Stability	26
6. Summary and Conclusions	30
Acknowledgement	32
References	33
Figures	35



Accession For	
NTIS CRA&I	<input checked="" type="checkbox"/>
DTIC TAB	<input type="checkbox"/>
Unannounced	<input type="checkbox"/>
Justification	
By _____	
Distribution/	
Availability Codes	
Dist	Available d/or Special
A-1	

List of Figures

	Page
Figure 1. Computational Grid (64x16) Around a Karman-Trefftz Airfoil	35
Figure 2. Hybrid Scheme--Initial Distribution of Pressure Coefficient on 64x16 Grid ($M_\infty = 0.63$; $\alpha = 2$ degrees; $C_L = 0.228$; $C_D = 0.020$)	36
Figure 3. Hybrid Scheme--Distribution of Pressure Coefficient on 64x16 Grid After 2400 Time Steps ($M_\infty = 0.63$; $\alpha = 2$ degrees; $C_L = 0.344$; $C_D = 0.009$)	37
Figure 4. Finite Volume Calculation--Distribution of Pressure Coefficient on 64x16 Grid ($M_\infty = 0.63$; $\alpha = 2$ degrees; $C_L = 0.3419$; $C_D = 0.0018$; $C_M = -0.0078$)	38
Figure 5. Hybrid Scheme--Distribution of Pressure Coefficient on 32x16 Grid ($M_\infty = 0.63$; $\alpha = 2$ degrees; $C_L = 0.333$; $C_D = 0.018$)	39
Figure 6. Hybrid Scheme--Initial Distribution of Pressure Coefficient on 64x16 Grid ($M_\infty = 0.7$; $\alpha = 2$ degrees; $C_L = 0.022$; $C_D = 0.002$)	40
Figure 7. Hybrid Scheme--Distribution of Pressure Coefficient on 64x16 Grid After 800 Time Steps ($M_\infty = 0.7$; $\alpha = 2$ degrees; $C_L = 0.411$; $C_D = 0.019$)	41
Figure 8. Hybrid Scheme--Distribution of Pressure Coefficient on 64x16 Grid After 1600 Time Steps ($M_\infty = 0.7$; $\alpha = 2$ degrees; $C_L = 0.323$; $C_D = 0.021$)	42
Figure 9. Hybrid Scheme--Isomach Lines in Flow Field on 64x17 Grid ($M_\infty = 0.7$; $\alpha = 2$ degrees)	43
Figure 10. Finite Volume Calculation--Distribution of Pressure Coefficient on 64x16 Grid ($M_\infty = 0.7$; $\alpha = 2$ degrees; $C_L = 0.3699$; $C_D = 0.0131$; $C_M = -0.0118$)	44
Figure 11. Finite Volume Calculation--Isomach Lines in Flow Field on 64x16 Grid ($M_\infty = 0.7$; $\alpha = 2$ degrees)	45
Figure 12. Hybrid Scheme--Distribution of Pressure Coefficient on 32x16 Grid ($M_\infty = 0.7$; $\alpha = 2$ degrees; $C_L = 0.362$; $C_D = 0.016$)	46
Figure 13. Chebyshev Method--Pressure Waves for One-Dimensional Problem Using 33 Grid Points	47

List of Tables

	Page
Table 1. Estimated Performance of Various Pseudospectral Schemes	20
Table 2. Numerical Results for Convergence of Iteration (Chebyshev Method)	25
Table 3. Fourier Iterative Implicit Method	29
Table 4. Chebyshev Iterative Implicit Method	29

1. Introduction

Pseudospectral methods have been used extensively in simulations of fluid flows (see, e.g., Orszag and Patera, 1983; Marcus, 1984; Riley and Metcalfe, 1979). The dependent variables are expanded in terms of a complete set of orthogonal functions defined in the computational domain. Either a Galerkin method or a collocation method can be employed to solve the governing partial differential equations. The basic numerical analysis of spectral methods has been reviewed in a monograph by Gottlieb and Orszag (1977). The advantage of the pseudospectral method over methods using locally supported basis functions, such as finite difference or finite element methods, is the fast convergence of the expansions, which results in a numerical scheme with very small dissipative and dispersive errors for solving partial differential equations. Application of the method to a compressible flow problem with shock waves has been studied in one-dimensional problems by Gottlieb et al. (1981) and Taylor et al. (1981). They demonstrated that a pseudospectral method can be used to capture shock waves in the flow field if an appropriate filtering technique is used to stabilize the computations and filter out the Gibb's oscillations.

With the developments to date, the pseudospectral method seems to offer the opportunity for a scheme superior to the finite difference method. Several problems need to be resolved, however, before a practical code can be constructed. Methods for filtering the Gibb's phenomenon associated with the shock wave must be studied, and the accuracy of the results after filtering must be critically examined. The application of pseudospectral methods to flows around a complex geometrical shape such as an airfoil has not been fully demonstrated. In particular, any geometrical singularity, e.g., the trailing edge of an airfoil, may cause difficulty for a global expansion method such as the pseudospectral method. The efficiency of pseudospectral computations as compared to those using a finite difference method must also be examined. To approach a steady state through time-marching calculations, a computational method allowing large time steps is preferred. An implicit pseudospectral scheme may be a good candidate for achieving this goal. A numerical analysis of an implicit scheme would give some insight into the efficiency of such a scheme.

These are the issues that are addressed in this report. Here, we present the results of our efforts to construct a hybrid scheme for computing

transonic flows around an airfoil. This hybrid scheme consists of a Fourier expansion in one direction and a finite difference scheme in the other direction. The application of various types of filters is examined through numerical experimentation. This work parallels a recent systematic study by Hussaini et al. (1985a) on the effects of various filters on the accuracy of Euler equation solutions using a Fourier method for one-dimensional problems. The efficiency of our pseudospectral computations as compared to those using a finite volume scheme is discussed. We also report the results of our attempt to construct a numerical scheme using spectral expansions in both directions. Finally, we present a numerical analysis of a Richardson iteration scheme for an implicit scheme. The analysis is supported by numerical experiments using a simple one-dimensional wave equation.

2. Governing Equations and Basic Approach

The equations governing inviscid, compressible flows are the Euler equations. For computing flows around an object with an arbitrary geometrical shape, a body-fitted computational coordinate system is used. If (x, y) represents a Cartesian physical coordinate and (X, Y) represents the computational space, then these equations can be written in strong conservation form by using contravariant velocities as follows:

$$\frac{\partial}{\partial t} (\vec{q}) + \frac{\partial}{\partial X} (\vec{F}) + \frac{\partial}{\partial Y} (\vec{G}) = 0 \quad (2.1)$$

where

$$\vec{q} = J \begin{bmatrix} \rho \\ \rho u \\ \rho v \\ E \end{bmatrix}; \quad \vec{F} = \begin{bmatrix} \rho U \\ \rho u U + y_Y P / \gamma M_\infty^2 \\ \rho v U - x_Y P / \gamma M_\infty^2 \\ \rho H U \end{bmatrix}; \quad \vec{G} = \begin{bmatrix} \rho V \\ \rho u V - y_X P / \gamma M_\infty^2 \\ \rho v V + x_X P / \gamma M_\infty^2 \\ \rho H V \end{bmatrix} \quad (2.2)$$

$$\begin{pmatrix} U \\ V \end{pmatrix} = \begin{pmatrix} y_Y & -x_Y \\ -y_X & x_X \end{pmatrix} \begin{pmatrix} u \\ v \end{pmatrix}; \quad H = [(\gamma-1)P + E] / \rho; \quad (2.3)$$

$$E = P + \frac{\gamma(\gamma-1)}{2} M_\infty^2 (\rho u^2 + \rho v^2);$$

ρ is the density of the gas; P is the pressure; (u, v) are the Cartesian components of the gas velocity; (U, V) are the unscaled contravariant velocity components associated with the curvilinear coordinates; J is the Jacobian of the transformation; E is the total energy; H is the specific total enthalpy; M_∞ is the freestream Mach number; and γ is the ratio between specific heat capacities. P , ρ and the Cartesian velocity components (u, v) are nondimensionalized by their freestream values; E and H are nondimensionalized by the freestream internal energy $C_v T_\infty$. The momentum equations as written in the above form compute the evolution of the Cartesian momentum components. Weak solutions with shock waves are allowed by the above equations, and entropy increases across the shock waves. The boundary conditions for these equations are the nonpermeable conditions on the solid surfaces and the assumption that disturbances generated by the airfoil are radiated to infinity with no reflection at the boundary of the computational domain. For steady-state calculations, it is hoped that the solution will be insensitive to the initial conditions specified.

The basic approach for applying the pseudospectral method to flows around an airfoil is described here. The exterior of an airfoil is mapped to the interior of a circle using a conformal mapping. Polar coordinates are used in the mapped plane. In the circumferential direction, we expand all variables in Fourier series because of the periodicity of the flow. In the radial direction, a Chebyshev polynomial expansion for all variables seems to be the natural choice because of its extensive use in other fluid mechanics calculations in a nonperiodic domain. In addition to the Chebyshev expansion, we have studied the polynomial subtraction method described by Gottlieb and Orszag (1977) and Roache (1978). In the numerical solution of a hyperbolic partial differential equation, the spatial discretization of the differential operators is accomplished by spectral expansions. Finite difference time discretization is used to advance the solution. Because of their convenience and computational efficiency, explicit time-stepping schemes are investigated first. Various methods for accelerating the convergence of the solution to a steady state are implemented. We also give an analysis of the implicit iterative schemes suggested by Gottlieb and Orszag (1977) by use of a simple one-dimensional model problem to explore the numerical properties of an implicit scheme.

3. Hybrid Scheme

When a conformal mapping is applied to map the exterior of an airfoil to the interior of a circle, a shock wave, which must be perpendicular to the airfoil surface for a transonic condition, will roughly align with a radial coordinate line in the mapped circle plane. Thus, it is reasonable to examine the capabilities of a pseudospectral method in resolving a shock wave by using a hybrid scheme that uses a Fourier series in the circumferential direction and a finite difference scheme in the radial direction. The use of the hybrid scheme allows the question of resolving a shock wave to be isolated from possible difficulties that may arise using Chebyshev series expansions. Techniques for filtering Gibb's ripples can also be studied. For these reasons, we have attempted to construct the hybrid scheme.

3.1 Spatial and Temporal Discretizations

The fluxes \vec{F} and \vec{G} in Equation (2.1) are computed in the physical space. Since all grid points are defined at equal intervals in the transformed space, the derivatives of the fluxes along the circumferential direction are evaluated by taking finite Fourier transforms of the fluxes, and inverse transforms are applied after the results are multiplied by the wave number. In the radial direction, a second-order central difference scheme is used to evaluate all derivatives. The resulting spatially discretized system is a system of ordinary differential equations in time.

Following Jameson et al. (1981), we use a four-stage Runge-Kutta scheme to advance the flow variables \vec{q} at the grid points. This time-stepping scheme is given by the following procedure:

$$\vec{q}^{(\ell)} = \vec{q}^{(0)} + \frac{1}{5-\ell} \vec{R}^{(\ell-1)} \Delta t ; \ell = 1, \dots, 4 \quad (3.1)$$

$$\vec{q}^{(0)} = \vec{q}^{(n)} ; \vec{q}^{(n+1)} = \vec{q}^{(4)} \quad (3.2)$$

where $\vec{R}^{(\ell-1)}$ is the residue evaluated by using $\vec{q}^{(\ell-1)}$.

The procedure requires only one level of memory for all variables and is exactly a fourth-order Runge-Kutta scheme for a linear equation. For a nonlinear equation, the procedure does not have the high-order time accuracy of the true Runge-Kutta scheme. However, we have chosen this scheme mainly

for the stability and not for the time accuracy. This simplified four-stage scheme serves our purpose well. For a one-dimensional simple wave equation, the scheme is stable for a CFL number of $2.8/\pi$ for a Fourier pseudospectral method as opposed to 2.8 for a finite difference method. For the hybrid scheme, the geometric average of the time step given by the finite difference scheme in the radial direction and that given by the spectral scheme in the circumferential direction is used. To avoid the severe constraint on the time step imposed by the small grid size near the trailing edge, we use a constant CFL number throughout the entire flow field. Thus, the time step at each grid point depends on the local grid size. The solution develops in a warped time domain. Again, the solution will not be time accurate. Only the steady-state solution is meaningful.

3.2 Boundary Conditions

It is well known that, for a hyperbolic system, one should take note of various characteristic variables preserved on the corresponding characteristics. Only the characteristic variables carried by the outgoing characteristics can be computed from the interior solution of the governing equations. The characteristic variables on the incoming characteristics must be replaced by the appropriate boundary conditions. Based on this principle, the following method of treating the boundary conditions is given.

There are four characteristics crossing the computational boundary. Two correspond to the acoustic waves with wave speed $(V_n \pm c)$, where V_n is the velocity component normal to the computational boundary. The other two are the vorticity mode and entropy mode, both with wave speed V_n . Let (V_s, V_n) be the flow speeds along and normal to the solid boundary, respectively. Then, the outgoing waves and the corresponding characteristic variables are

$$\begin{aligned}
 P_c - \gamma M_{\infty}^2 \rho_c V_{nc} & \text{ on } -c \\
 V_{sc} & \text{ on } V_n = 0 \\
 P_c + \gamma M_{\infty}^2 \rho_c C^2 & \text{ on } V_n = 0
 \end{aligned}
 \tag{3.3}$$

where the subscript c denotes the variables computed from the interior algorithm. These characteristic variables are linearized with respect to the flow variables at the previous time step.

By using the boundary condition $V_n = 0$ together with the characteristic variables from Equation (3.3), the conservations of characteristic variables along the characteristic line give the following equations for the flow variables on the boundary points:

$$\begin{aligned}
 P - \gamma M_{\infty}^2 \rho_c C V_n &= P = P_c - \gamma M_{\infty}^2 \rho_c C V_{nc} \\
 \rho &= \rho_c + \frac{1}{\gamma M_{\infty}^2 C^2} (P - P_c) \\
 V_s &= V_{sc} \\
 V_n &= 0
 \end{aligned}
 \tag{3.4}$$

Other flow variables, such as ρu , ρv , E and H , can be recovered from the results obtained above.

On the far-field boundary, flows are only slightly perturbed from the freestream condition. The Riemann invariants are used to compute the flow variables on the boundary. For the Riemann invariant on the outgoing characteristics, extrapolation from the interior points is used, while the free-stream value is used for the Riemann invariant on the incoming characteristics. After the normal velocity and the speed of sound are computed, the velocity tangential to the boundary is computed by the freestream value and the perturbed value based on the far-field solution of a circulation around the airfoil. The rest of the flow variables are computed by the isentropic relations. We have attempted other boundary treatments using a full characteristic set similar to that applied at the outer boundary. The results of computations do not seem to change substantially.

3.3 Convergence Acceleration

The stability criterion for the numerical scheme described is approximately $2.8/\pi$. For a steady-state computation, this requires excessive computing time. To increase the time step of the computation, the residue-smoothing technique developed by Jameson and Baker (1983) is applied to the scheme as discussed below.

Let the time change of the flow variables be R . For steady-state computations, it is desirable to drive R to zero. Let L be a nonsingular linear operator and \bar{R} be defined as

$$L\bar{R} = R \quad \text{or} \quad \bar{R} = L^{-1}R \quad . \quad (3.5)$$

If \bar{R} can be driven to zero by advancing in time, using \bar{R} as the time change of the flow variables, it automatically ensures that R becomes zero. Now, R is a residue defined by a pseudospectral spatial expansion of the variables, then vanishing \bar{R} still ensures spectral accuracy of the scheme even if L is not a spectral operator. The choice of L is to improve the stability of the numerical scheme. It has been shown by Jameson and Baker that the following operator serves the purpose:

$$L = (1 - \epsilon\delta_X^2)(1 - \epsilon\delta_Y^2) \quad (3.6)$$

where δ_X and δ_Y are finite difference operators in the transformed coordinates (X, Y) . To understand the reason for improved stability for a pseudospectral scheme, a simple one-dimensional wave equation is considered:

$$\phi_t + c\phi_x = 0 \quad . \quad (3.7)$$

The residue-smoothing process as described is equivalent, to the lowest order, to adding an additional term to the original simple wave equation and converting it to the following equation:

$$\phi_t + c\phi_x - \epsilon(\Delta x)^2 \phi_{txx} = 0 \quad . \quad (3.8)$$

The dispersion relation for this equation can be given as

$$\frac{\omega}{k} = \frac{c}{1 + \epsilon k^2 (\Delta x)^2} \quad (3.9)$$

where ω is the frequency and k is the wave number. By increasing the parameter ϵ , the wave speed for the high-wave-number component is substantially reduced. This reduction in wave speed for the dangerous short waves contributes to the increase in the time step size. Equation (3.8) is the linearized form of a model equation for long dispersive waves proposed by Benjamin et al.

(1972). They pointed out the numerical advantage of using this equation over the Kortweg-de-Vries equation. Other means of manipulating the dispersion relation to gain stability have been suggested (see Gottlieb and Turkel, 1980, for example). However, these methods do not preserve the original conservation laws as their limit in steady state.

In principle, the method described above can be stable for any desired time step if a large enough ϵ is chosen. In practice, the approach to steady state can be delayed if a large ϵ is chosen. We take $\epsilon = 1.5$, and the CFL can be increased 50% from its original value. Beyond this value, it does not seem to help the approach to steady state.

3.4 Filter and Artificial Viscosity

The above scheme by itself is unstable due to the buildup of high-frequency components of error. In the finite difference scheme, a form of artificial viscosity has been suggested by Jameson et al. (1981) for incorporation into a central difference scheme. Sakell (1984) has chosen second-order and fourth-order viscosity in his study of pseudospectral schemes. It is well known that the use of artificial viscosity will broaden the shock thickness. The objective of using a pseudospectral method to better resolve the shock wave is thus defeated. Furthermore, we have experimented with the artificial viscosity using the form given by Jameson et al. (1981). We have found that the amount suggested by Jameson et al. is not sufficient to control the Gibb's phenomena, and the amount must be increased to obtain a stable calculation. This increase further broadens the shock wave to an unacceptable level. For this reason, we have decided to use the artificial viscosity in Jameson's form only in the radial direction, along which a finite difference discretization has been used. In the circumferential direction, another kind of filter must be used.

We have conducted a systematic experiment with various types of filters for pseudospectral transonic calculations. Our experience is summarized here.

High Wave-Number Cutoff

After advancing a time step, the flow variables are expanded into Fourier series. The coefficients of the highest 10% wave numbers are set to zero. It is found that the time marching cannot be stabilized. The intermediate solutions also show that the shock resolution has deteriorated. The method is

equivalent to adding artificial viscosity terms of even order to the conservation equations. Other filters in wave-number space have similar properties and do not stabilize the solution. Similar conclusions were obtained by Hussaini et al. (1985). A point worth mentioning is that the solution in the present scheme is advanced in the physical space as opposed to advancing the Fourier coefficients in time. Filtering in the spectral space requires additional finite Fourier transforms of all flow variables. The operation count of the computation is substantially increased.

Derivative Filtering

As will be discussed later (Section 3.5), the residue of the pseudospectral scheme does not decrease monotonically during time marching for steady-state computations. One of the reasons is the Gibbs' error in evaluating spectrally the derivatives of the fluxes. Consider a step function in physical space. The derivatives are zero everywhere. By using finite Fourier transforms to evaluate the derivatives, a large error is committed near the discontinuity. We have attempted to filter the derivatives of the fluxes in the spectral space when forming residue in the hope of obtaining a better estimate. The numerical experiments show that this type of filtering cannot stabilize the computations.

One-sided Schumann Filter

Another form of filtering is to average the flow variables around the grid point. In one dimension, this takes the following form:

$$\vec{q}_i = 0.25 (\vec{q}_{i+1} + 2\vec{q}_i + \vec{q}_{i-1}) \quad . \quad (3.10)$$

To avoid smearing shock waves, the sonic points at the shock are located on each coordinate line around the airfoil. The following one-sided averaging is applied on each side of the shock wave.

$$\vec{q}_i = 0.5 (\vec{q}_i + \vec{q}_{i+1}) \quad (3.11)$$

This filter has been suggested by Gottlieb et al. (1981). If applied at each time step, it is equivalent to a first-order-accurate second-order artificial viscosity. We have applied this filtering once every L time steps, just often

enough to damp the instability. It is believed that this application of the filter reduces the error. This filter has been found to be the most effective in stabilizing the calculations. The amount of artificial viscosity is roughly of the order of

$$\frac{(\Delta x)^2}{4(L\Delta t)} \quad (3.12)$$

Assuming that $L\Delta t$ is of $O(1)$ as in the present investigation, the artificial viscosity is of the order of $(\Delta x)^2$ in contrast to $(\Delta x)^3$ for the form suggested by Jameson et al. (1981). As has been discussed, the form of artificial viscosity suggested by Jameson et al. is not sufficient to stabilize the pseudo-spectral computation. It seems that a lower order filter such as the present one is required. The advantage of the present filter is that the sharpness of the shock wave can be maintained.

3.5 Computed Results

Test calculations were performed for the flow around a Karman-Trefftz airfoil. An analytic transformation that maps the interior of a circle in the computational space ζ to the exterior of an airfoil in the physical space Z is given as follows:

$$\frac{Z}{\kappa l} = \frac{(1+l\zeta)^\kappa + (1-l\zeta)^\kappa}{(1+l\zeta)^\kappa - (1-l\zeta)^\kappa} \quad (3.13)$$

with

$$l = (1 - \eta_0^2)^{1/2} - \xi_0 \quad (3.14)$$

where $\zeta_0 = (\xi_0, \eta_0)$ is the coordinate of the center of the circle in the ζ plane. For the present example, $\zeta_0 = (-0.1, 0)$. At the trailing edge, this transformation is singular. In the present investigation, the trailing edge is placed at the half grid between grid points to avoid the singularity. The coordinates of the grid points in the physical space are computed from the transformation, and the transformation matrices are computed at each grid point using exactly the same algorithm for the evaluation of flux derivatives. These matrices are stored to save computational time. Figure 1 shows the computational grid around the airfoil.

The computations start from an incompressible velocity field determined by the conformal mapping. The density and pressure fields are given by the isentropic relations. The lift and drag coefficients are computed by integrating the pressure around the airfoil. To be consistent with the pseudospectral numerical scheme, the integrals have been performed by using a Fourier series expansion of the surface pressure as follows:

$$\vec{F} = -\oint P \vec{n} ds = -\oint \left[P y_X \Big|_{Y=0} \vec{i} - P x_X \Big|_{Y=0} \vec{j} \right] dx \quad (3.15)$$

Let

$$\begin{aligned} -P y_X \Big|_{Y=0} &= f_x \\ P x_X \Big|_{Y=0} &= f_y \end{aligned} \quad (3.16)$$

Then the force $\vec{F} = (F_x, F_y)$ is simply the coefficients a_{ox} and a_{oy} of the Fourier expansion for f_x and f_y .

A transonic case with a freestream Mach number of 0.63 and an angle of attack of 2 degrees is computed. The computations are done on both a 64x16 grid and a 32x16 grid. Figure 2 shows the initial distribution of the pressure coefficient on the denser grid, and Figure 3 shows the solution after 2400 time steps. The pressure distribution essentially remains constant after 1800 time steps. Figure 4 shows the results of a computation using the finite volume code FLO53 with the same grid density. Notice that a weak shock wave appears on the pseudospectral calculation. The same case is computed on a 32x16 grid, and the results are shown in Figure 5. The results indicate that, although the 32x16 grid gives the gross features of the pressure distribution, the solution is not accurate enough. The drag count for the spectral calculations seems to be too large for this low supercritical case, which may be due to the error introduced by the filtering.

A supercritical case with a freestream Mach number of 0.7 and an angle of attack of 2 degrees has also been computed on the 64x16 grid. Figures 6 through 8 show the pressure distributions after 0, 800, and 2400 time steps, respectively. The solution seems to reach a steady state in 1600 time steps. This is approximately equivalent to the 500 time steps required in the finite volume computation if we take into account the ratio of π between the

time steps for the two methods to satisfy the stability requirements. The shock wave is resolved in one grid. Figure 9 shows the isomach lines in the flow field. Figures 10 and 11 show the results from a finite volume calculation on the same grid. The shock resolution is not as good as in the spectral calculation. We have performed a finite difference calculation with a central difference scheme in the circumferential direction. By using the same filter as in the pseudospectral calculation, we intend to determine whether the shock resolution is the result of the particular filter or the result of pseudospectral discretization. The finite difference calculation diverges, which seems to indicate the merit of the spectral scheme. Figure 12 shows the results of a 32x16 computation using the hybrid scheme. Again, it gives the correct gross features of the flow field, while the finite volume scheme on the same grid gives unacceptable results with a smeared shock wave.

The results of the computations can be summarized as follows:

- (1) The shock wave can be resolved within one grid using the hybrid scheme, while it takes three to four grids for the finite volume code. The best upwind finite difference codes (Anderson et al., 1985; Yee, private communication, 1985) can resolve a shock wave within two grids.
- (2) The accuracy in the smooth flow region seems to be deteriorated by the filter being used. The expansion on the lower surface is probably not accurate enough, and the drag count is too high.
- (3) The residue in computations does not decrease with time. The residue decreases first and then starts to diverge. At this point, the Schumann filter is applied, and the residue resumes its decreasing trend. The computation is a slowly divergent one stabilized by periodic filtering. Hence, it is very difficult to decide the steady-state solution. In fact, for supercritical cases, the variation of the number of supersonic points is used as an indicator for steady state.
- (4) The computations with the pseudospectral scheme require more time steps to reach a steady state due to the smaller time steps required by the CFL restriction. To compute the supercritical lifting case

presented in the present report, 1800 time steps are required as opposed to 500 time steps for the finite volume scheme with the same number of grid points. The ratio is roughly π as indicated by the stability analysis. The additional number of time steps can be justified only if the pseudospectral calculations can reduce the number of grid points by a factor of 4. Another possibility, which was not investigated here, is to use a multigrid method in conjunction with the pseudospectral method to reduce the number of work cycles.

These examples show that the pseudospectral method may not be competitive with the finite difference methods for steady-state problems with shock waves. The ability of the pseudospectral calculations to resolve a shock wave in one grid does not justify the excessive computing time required. Spectral accuracy is destroyed by the existence of discontinuity. Since the Gibb's error is a systematic error, one would hope that the spectral accuracy can be restored by a proper filtering technique. The filters examined in the present work fail to accomplish this purpose.

4. Development of a Fully Spectral Method

In this section, we describe the results of an effort to extend the method to include a spectral expansion in the radial direction in the computational space. If successful, the scheme will be a fully spectral scheme with high accuracy in both directions.

Chebyshev polynomial expansions have been extensively used in the simulations of incompressible viscous flows (see, e.g., Orszag and Patera, 1983; Marcus, 1984). Application of the Chebyshev method to compressible flows using the full potential equation has been investigated by Streett (1983). Hussaini et al. (1985b) used this method in conjunction with a shock-fitting method to study the interactions between a shock wave and a hot spot. They have shown that the Chebyshev method is highly accurate in that case. The application of the method to a steady-state compressible flow using a shock-capturing, Euler equation, time-marching technique has been investigated by Gottlieb et al. (1984). It seems to be a natural choice for developing a fully spectral scheme.

A polynomial subtraction Fourier method has been suggested by Gottlieb and Orszag (1977). Roache (1978) studied the accuracy of the method in conjunction with the degree of the polynomial used. Orszag and Patera (1983) used the method for simulations of incompressible viscous flows. We shall investigate the possible application of the method to the present case.

4.1 Fourier Chebyshev Method

In the unit circle computational plane, the dependent variables are expanded into a finite Fourier series in the circumferential direction and a Chebyshev series in the radial direction. In the radial direction, the computational domain $(\epsilon, 1)$ is divided into $(N+1)$ unequal Chebyshev collocation points. In the present work, the collocation method is used.

Derivatives of Fluxes

The fluxes are computed at the grid points. The radial derivatives of the fluxes are computed by a finite Chebyshev expansion of these data. Due to the nature of the transformation, the fluxes are singular at the center of the circle. The singularity behaves as follows:

$$(\vec{F}, \vec{G}) \sim \vec{K}/Y \quad (4.1)$$

where \vec{K} is the strength of the singularity. Although the far-field boundary is chosen at a finite distance $Y = 0.02$, substantial errors are committed in the spectral evaluations of the derivatives of fluxes due to the inability of the finite series to sufficiently resolve the singularity if 17 or fewer grid points are used. As a result, ripples occur in the evaluated derivatives. These ripples are not confined to the far field but also propagate to the near field. To reduce these ripples, we have subtracted a singular function from the radial flux vectors as follows:

$$\vec{G}' = \vec{G} - \vec{K}/Y \quad (4.2)$$

where \vec{K} is determined by the fluxes at the first two points in the far field. The reduced fluxes G' are expanded in Chebyshev series. The spatial derivatives of G are obtained by the combination of the derivatives of G' and the singular term. This method has proven to eliminate the ripples in the evaluation of derivatives by Chebyshev series. However, the process increases the computational overhead.

Stability and Convergence to Steady State

The following formula defines the Chebyshev collocation points for an N -term series:

$$Y_j = \frac{(1 - \epsilon_0)}{2} \left[1 - \cos \frac{\pi(j-1)}{N} \right] + \epsilon_0 ; j = 1, \dots, N+1 \quad (4.3)$$

These points are close together near the boundary with spacing of $O(N^{-2})$.

The stability requirement is

$$\Delta t = O \left[\frac{1}{N^2(U+C)} \right] \quad (4.4)$$

where the characteristic velocity is $(U+C)$. The computational time required to reach a steady state is increased by a factor of N as compared to that using an equally spaced Fourier method. This is in contrast to the incompressible viscous simulations, where the characteristic velocity approaches zero on the boundary. The time steps can maintain a reasonable value even with a highly stretched grid, like the Chebyshev collocation grid in that case.

The residue-averaging technique and the use of local time steps, as described in the previous section for the hybrid scheme, fail to improve the

convergence. To understand the performance of the Chebyshev method in a compressible flow, particularly with the boundary conditions, we have tested a wave propagation problem in one dimension. The Euler equations are solved in one dimension with a smoothed pressure discontinuity, isothermal and no flow as initial conditions. The pressure difference across the wave is 2. We are interested in the time step size and the effects of boundary conditions on the stability of the computations. Figure 13 shows the results of computation using 33 grid points. In order to maintain stability, the time step is so small that it takes 4800 time steps for the pressure wave to propagate across half the computational domain. The boundary treatment does produce shock reflection on the solid boundary. The main conclusion obtained here is that unless an acceleration scheme can be found to drive effectively the solution to steady state, the Chebyshev explicit method is not suitable for steady-state calculations. Since the use of a local time step and residue averaging fails to stabilize the calculations, an implicit method may be the solution to the problem. This is the reason we have decided to investigate an implicit iterative scheme, as described in Section 5.

4.2 Polynomial Subtraction Method

To circumvent the difficulty of the Chebyshev method as discussed above, we have experimented with a polynomial subtraction Fourier method.

Let G be the flux vector. The computational space $(\epsilon, 1)$ is divided into N equally spaced grids. Consider a reduced flux vector \vec{G}' defined as

$$\vec{G}' = \vec{G} - \vec{K}/Y - \vec{P}_m(Y) \quad (4.5)$$

where \vec{K} is the strength of the singularity at $Y = 0$ as defined in the previous section and \vec{P}_m is a polynomial of m th degree. One can construct a polynomial P_m in such a way that G' is periodic at the boundaries up to the $(m-1)$ th derivatives at its boundaries. The derivatives of the flux vector \vec{G} can be reconstructed by using the Fourier spectral method on G' and analytical expressions for the other two terms.

Accuracy of the Method

Since the method only eliminates the discontinuity of \vec{G} up to the $(m-1)$ th order, the resulting Fourier series converges as $N^{-(m+1)}$. For example, if a third-order polynomial is used, the first discontinuity at the boundaries is the third derivative. The resulting Fourier method is fourth-order accurate. This estimation is based on the assumption that the 'jumps' of the derivatives of G at the boundaries are known exactly. In the present problem, these 'jumps' must be evaluated by approximate means. The error committed in the evaluation of the jumps must be consistent with the order of the polynomial being used.

Construction of Polynomial P_m

In order to construct P_m , the jumps in the derivatives of the flux vector G up to the $(m-1)$ th order at both ends of the finite domain are required. Since G is known only at the discrete points, the evaluation of these derivatives can only be achieved by using a finite difference method. The truncation error in this process will also affect the accuracy of the method. For example, when a second-order one-sided differencing is used to evaluate the end point derivatives, the jump in the first-order derivative of the reduced flux G' at the boundary is of $O(\Delta x^2)$. Since the $O(1)$ jump in the first-order derivative results in $O(N^{-2})$ convergence in the Fourier series, the resulting polynomial subtraction method is of $O(N^{-4})$. Hence, it is consistent to use a second-order-accurate evaluation of the jump in conjunction with the use of a third-order polynomial.

Computational Experiments

We have experimented with the method using a third-order polynomial. A computation with the same supercritical case computed earlier using the hybrid scheme is carried out. The time step for the 'full spectral' calculations is half that for the hybrid scheme. The computations produce similar results to the hybrid scheme, with computational time more than double that of the hybrid scheme. We have decided that the method is not competitive with a hybrid scheme with twice the number of grid points in the radial direction.

5. Implicit Pseudospectral Method

There are two reasons why we would like to examine an implicit method. First, as discussed in the previous sections, there are several problems in using explicit schemes for pseudospectral Euler equation calculations. One of the most difficult problems with these schemes is the small time steps required by the stability criteria. The Chebyshev method, in particular, requires extremely small time steps. An implicit method may free us from this constraint. The other reason is to construct an implicit method for time-accurate unsteady calculations. Consider the flow around an airfoil. The grid size near the leading and trailing edges is extremely small. For an unsteady calculation, one cannot use the local time step as described in Section 3. An implicit method is essential in this case to avoid excessive computing time.

Table 1 summarizes the performance of various pseudospectral schemes for the wave equation

$$u_t + u_x = 0 \quad . \quad (5.1)$$

It can be seen that an operation count of $O(N^4)$ is required for all implicit methods if a direct inversion method is used. Since the pseudospectral method gives a full matrix operation on the variables at grid points, a sparse matrix technique for inverting the operator is not applicable.

We shall examine an iterative implicit method that uses a finite difference operator as an approximate operator for the spectral operator for the iteration. If there exists a stable and convergent iterative scheme, the work required for such a scheme will be

$$W = MN^2 \log N \quad (5.2)$$

where N is the number of modes and M is the number of iterations per time step. Here, we have assumed that $N\Delta t = O(1)$ for time accuracy, and for each iteration the operation count is roughly that required by an explicit scheme, i.e., the overhead on inverting an approximate operator is neglected. Therefore, the Chebyshev implicit iterative method will have better performance than the explicit method if M is much less than $O(N)$. For a steady-state calculation where it is possible to have $N\Delta t \gg 1$, the method can also improve the performance of a Fourier scheme.

Table 1. Estimated Performance of Various Pseudospectral Schemes

Spectral Method	Time Discretization	Accuracy $O(\Delta t^k)$	Stability	Work to Reach $t = T$
Fourier	Leap Frog	2	$\frac{1}{\pi}$	$2\pi N^2 \log N$
Fourier	Crank-Nicolson	2	Stable	$N^{4/3}$
Fourier	Forward Euler	1	C/N	$\frac{N^3}{C} \log N$
Fourier	Backward Euler	1	Stable	$N^{4/3}$
Fourier	2-step Runge-Kutta	2	$C/N^{1/3}$	$\frac{2N^{7/3}}{C} \log N$
Fourier	3-step Runge-Kutta	3	$\frac{\sqrt{3}}{\pi}$	$2\pi\sqrt{3} N^2 \log N$
Fourier	4-step Runge-Kutta	4	$2\frac{\sqrt{2}}{\pi}$	$2\pi\sqrt{2} N^2 \log N$
Chebyshev	Leap Frog	2	Unstable	----
Chebyshev	Adams-Bashforth	2	4/N	$\frac{N^3}{4} \log N$
Chebyshev	Crank-Nicolson	2	Stable	$N^{4/3}$
Chebyshev	Backward Euler	1	Stable	$N^{4/3}$

We shall examine a Richardson iteration scheme in this section. Two problems regarding the iterative scheme are addressed here: What is the best way to construct a scheme that will converge quickly at each time step? Is the time-stepping scheme stable if only a finite number of iterations at each time step are carried out? These problems are addressed through the numerical analysis of a simple wave equation and numerical experiments to substantiate the theory.

5.1 Richardson Iteration

Consider the simple wave equation

$$\frac{\partial u}{\partial t} + \frac{\partial u}{\partial x} = 0 \quad . \quad (5.3)$$

In finite dimensional space, we approximate the above equation by the following backward Euler pseudospectral scheme:

$$(I + \Delta t A) u^{n+1} = u^n \quad (5.4)$$

where n denotes the time level, A represents the spectral approximation of the operator $\partial/\partial x$, and u^{n+1} is obtained by inverting $(I + \Delta t A)$ and operating the results on the known quantity u^n . The algebraic equation, in a simple form, can be written as

$$Lu = f \quad (5.5)$$

where

$$L \equiv (I + \Delta t A) \quad (5.6)$$

$$u \equiv u^{n+1} \quad (5.7)$$

$$f \equiv u^n \quad (5.8)$$

Let L_{ap} be an approximate operator to L that can be inverted easily. Then an iterative scheme is suggested as

$$L_{ap} (u_{m+1} - u_m) = -\alpha(Lu_m - f) \quad (5.9)$$

or

$$u_{m+1} = (I - \alpha L_{ap}^{-1} L) u_m + \alpha L_{ap}^{-1} f \quad (5.10)$$

where α is a parameter that can be adjusted to enhance the convergence. The iteration will converge if

$$K \equiv \left\| I - \alpha L_{ap}^{-1} L \right\| \leq 1 \quad . \quad (5.11)$$

Let B be the central finite difference approximation of $\partial/\partial x$. We choose

$$L_{ap} \equiv (I + \Delta t B) \quad (5.12)$$

as an approximate operator to L. The original backward Euler time-step pseudospectral scheme can be solved by the following iterative scheme:

$$(I + \Delta t B) u_{m+1} = \alpha u^n + (1 - \alpha) u_m + \Delta t (B - \alpha A) u_m. \quad (5.13)$$

5.2 Convergence of Richardson Iteration

The convergence property of the Richardson iteration scheme presented above is examined here. In particular, we shall attempt to derive an expression for the optimum parameter α in terms of the spectral properties of the operators L and L_{ap} .

Let $\epsilon_m = u_m - u$. Then, from Equation (5.10),

$$\|\epsilon_{m+1}\| \leq \max(|1-\alpha s|, |1-\alpha S|) \|\epsilon_m\| \quad (5.14)$$

where s and S are the bounds of the operator $L_{ap}^{-1}L$ defined on a smooth test function x as

$$0 < s \leq \frac{\|L_{ap}^{-1}Lx\|}{\|x\|} \leq S < \infty; \quad N \rightarrow \infty. \quad (5.15)$$

Optimum convergence is given by

$$\alpha_{opt} = \frac{2}{s + S}, \quad (5.16)$$

and the corresponding convergence rate is given by

$$K_{opt} = \frac{S - s}{S + s} < 1. \quad (5.17)$$

The bounds s and S must be estimated. Let $D \equiv L_{ap}^{-1}L$ and

$$DD^T Z = \lambda Z \quad (5.18)$$

where

$$\|Z\| = 1.$$

Then

$$s \leq \lambda_{min}^{1/2} \quad (5.19)$$

$$S \geq \lambda_{max}^{1/2}. \quad (5.20)$$

From Equation (5.18), it is easy to show that

$$LL^T Z = \lambda L_{ap} L_{ap}^T Z \quad (5.21)$$

Hence

$$\lambda = \frac{(LZ, LZ)}{(L_{ap} Z, L_{ap} Z)} \quad (5.22)$$

Using the definitions given by Equations (5.6) and (5.12), we have

$$\lambda = \frac{\{1 + \Delta t [(A+A^T)Z, Z] + \Delta t^2 (AZ, AZ)\}}{\{1 + \Delta t [(B+B^T)Z, Z] + \Delta t^2 (BZ, BZ)\}} \quad (5.23)$$

For the Fourier method and central difference scheme,

$$A^T = -A \quad (5.24)$$

$$B^T = -B \quad (5.25)$$

and

$$\lambda = \frac{1 + \Delta t^2 (AZ, AZ)}{1 + \Delta t^2 (BZ, BZ)} \quad (5.26)$$

Assume that sharp bounds exist:

$$\begin{aligned} b^2 N^2 \leq (BZ_{\max}, BZ_{\max}) &\leq \|B\|^2 \\ (AZ_{\max}, AZ_{\max}) \leq a^2 N^2 &\leq \|A\|^2 \end{aligned} \quad (5.27)$$

Then

$$S = \left[\frac{1 + (aN \Delta t)^2}{1 + (bN \Delta t)^2} \right]^{1/2} \quad (5.28)$$

For the Fourier method, Gottlieb and Orszag (1977) show that

$$(AZ, AZ) \geq (BZ, BZ) \quad \forall Z \quad (5.29)$$

Since B is an approximation of A,

$$AZ_{\min} \approx BZ_{\min}$$

and

$$s \approx 1, \quad (5.30)$$

then

$$S \rightarrow a/b \text{ as } N\Delta t \gg 1. \quad (5.31)$$

Since Gottlieb and Orszag (1977) show that the maximum eigenvalue of A is π times the maximum eigenvalue of B, then the scheme will not converge for $\alpha = 1$. From Equations (5.16) and (5.17), we have

$$\alpha_{\text{opt}} \rightarrow \frac{2(b/a)}{1 + b/a} \quad (5.32)$$

$$K_{\text{opt}} \rightarrow \frac{1 - b/a}{1 + b/a} \quad (5.33)$$

Note that the optimum convergence is independent of N in the limit $N\Delta t \gg 1$. Similar conclusions can be obtained for the Chebyshev method.

The following numerical experiments have been conducted to test the above theory for convergence of the iteration scheme. The Chebyshev collocation method is used.

A smoothed step function is chosen as an initial condition. An arbitrary parameter α is chosen. Two computations are made with different time step sizes, Δt_1 and Δt_2 . From the convergence rate, one can compute the bounds S_1 and S_2 . By using Equation (5.28), the parameters a and b can be computed. They are then substituted into Equations (5.28), (5.16) and (5.17) to obtain the theoretically computed optimum parameter α_{opt} and convergence rate K_{opt} . These are given for various numbers of modes and different CFL numbers in the right-hand columns of Table 2. To verify the theoretical results, α is varied for fixed N and $N\Delta t$ until optimal convergence is achieved. The experimentally obtained α_{opt} and K_{opt} are also given in the same table. The theoretical values show good agreement to the experimental values. The optimal convergence rate K_{opt} varies with the CFL number for fixed N but is almost independent of N for $N\Delta t = 2$ as concluded above. However, slow convergence for high CFL numbers does not imply higher computational costs, since fewer time steps are required to reach a specific time. The gain in computational effort will be addressed later.

Table 2. Numerical Results for Convergence of Iteration
(Chebyshev Method)

Number of Modes, N	CFL = $N\Delta t$	Numerical Experiments		Theoretical Values	
		α_{opt}	K_{opt}	α_{opt}	K_{opt}
16	0.4	0.80	0.27	0.86	0.28
16	0.8	0.70	0.38	0.74	0.38
16	1.0	0.65	0.43	0.69	0.43
16	2.0	0.40	0.59	0.51	0.63
32	0.4	0.70	0.34	0.74	0.37
32	0.8	0.60	0.43	0.57	0.43
32	1.0	0.50	0.47	0.51	0.47
32	2.0	0.30	0.67	0.36	0.68
64	0.4	0.60	0.37	0.57	0.38
64	0.8	0.50	0.47	0.41	0.52
64	1.0	0.40	0.54	0.36	0.57
64	2.0	0.27	0.69	0.27	0.69

5.3 Finite Iteration Stability

The above section addressed the question of convergence at each time step. Here, we examine the stability of the time-stepping scheme with finite Richardson iterations.

Consider again Equation (5.5) and the iterative implicit scheme, Equation (5.10). For a finite M-step iteration, the time stepping is

$$u_M = K^M u_0 + \alpha \sum_{m=0}^{M-1} K^m L_{ap}^{-1} f \quad (5.34)$$

where u_0 is the initial guess for the iteration and

$$K = I - \alpha L_{ap}^{-1} L \quad (5.35)$$

Since

$$\sum_{m=0}^{M-1} K^m = (I - K)^{-1} (I - K^M) \quad (5.36)$$

and

$$L_{ap} K^m L_{ap}^{-1} = L K^m L^{-1} \quad (5.37)$$

Equation (5.34) can be written as

$$u_M = L^{-1} f + K^M (u_0 - L^{-1} f) \quad (5.38)$$

The factor in the parentheses is simply the error of the initial guess u_0 and is denoted by ϵ_0 so that

$$u_M = u + K^M \epsilon_0 \quad (5.39)$$

Let us first choose an extreme example of $u_0 = 0$. Equation (5.38) can then be written as

$$u^{n+1} = G u^n \quad (5.40)$$

where

$$G = (I - K^M) L^{-1} \quad (5.41)$$

For stability, we must have

$$\|G\| \leq 1 \quad (5.42)$$

This implies that

$$||K||^M \leq \rho_{\min}(L) - 1 \quad (5.43)$$

where $\rho_{\min}(L)$ is the spectral radius of L . The estimates for the spectral radius (Gottlieb and Orszag, 1977) are

$$\rho_{\min}(L) - 1 = \begin{cases} CN^{-1/2} & \text{Chebyshev} \\ CN^{-1} & \text{Fourier} \end{cases} \quad (5.44)$$

with

$$\Delta t = O(N^{-1}).$$

Since, for large $N\Delta t$, $||K||$ is independent of N as discussed in the previous section, Equation (5.43) implies that

$$M \geq O(\log N) \quad (5.45)$$

for convergence.

Next, consider that the initial guess at each time step is given by the solution predicted by a forward Euler step

$$u_0 = (I - \Delta t A) u^n \quad (5.46)$$

It can be shown that the amplification factor is given by

$$G = \{K^M \Delta t^2 A^2 + I\} L^{-1} \quad (5.47)$$

The stability criterion now gives

$$||K||^M \leq \frac{\rho_{\min}(L) - 1}{\Delta t^2 \rho_{\min}(L) \rho_{\max}(A^2 L^{-1})} \quad (5.48)$$

But

$$\rho_{\max}(A^2 L^{-1}) = \begin{cases} O(N^2) & \text{Chebyshev} \\ O(N) & \text{Fourier} \end{cases} \quad (5.49)$$

The stability requires

$$M \geq \begin{cases} O(\log N) & \text{Chebyshev} \\ O(1) & \text{Fourier} \end{cases} \quad (5.50)$$

These examples show that the Richardson implicit method can improve the Chebyshev method in terms of computational efficiency.

Numerical experiments have been carried out to substantiate these analyses. The Fourier method is applied to solve the simple wave equation with the periodic initial condition in (0, 1):

$$u(x, 0) = \begin{cases} 1 & |x-1/2| \leq 1/4 \\ 0 & |x-1/2| > 1/4 \end{cases} \quad (5.51)$$

The initial condition is smoothed by averaging the u value of the neighboring points twice using

$$\bar{u}_i = \frac{1}{4} (u_{i+1} + 2u_i + u_{i-1}) \quad (5.52)$$

The optimal iteration parameters α_{opt} are chosen according to the results given in the previous section. For each time step, the iteration is terminated by the condition

$$\|u_{m+1} - u_m\| \leq \sigma \|u_m - u_e\| \quad (5.53)$$

where u_e is the solution given by the forward Euler step and σ is the tolerance parameter. Table 3 summarizes the results of the numerical experiments for the Fourier method. The implicit iterative scheme is stable for large CFL numbers as compared to the explicit method. However, the computational time can be larger than that using an explicit scheme due to the large number of iterations required for each time step. For the Fourier method, the iterative scheme does not offer any advantages over an explicit scheme.

We now turn to the Chebyshev method. Table 4 summarizes the numerical results. The performance of the explicit scheme is very poor, as can be seen from the table. For 64 modes, the method diverges even with a CFL number of 0.0125. The improvement in both accuracy and efficiency with an iterative implicit scheme is very much evident. Savings by a factor of 8 can be seen for a 32 mode calculation. For 64 modes, the iterative implicit method is stable for a CFL number of 1.0.

Table 3. Fourier Iterative Implicit Method

N	CFL	L ₂ Error Norm e	CPU/T
16	0.4	0.54-1	1.4
16	1.0	0.51-1	1.2
16*	0.1	0.55-1	1.3
32	0.4	0.27-1	6.1
32	1.0	0.30-1	11.0
32*	0.1	0.28-1	5.9
64	0.4	0.13-1	35.0
64	1.0	0.19-1	61.0
64*	0.1	0.15-1	26.0

*Explicit Leap-Frog Scheme

Table 4. Chebyshev Iterative Implicit Method

N	CFL	L ₂ Error Norm e	CPU/T
16	0.4	0.33-1	2.1
16	1.0	0.27-1	1.6
16*	0.1	0.33-1	3.9
32	0.4	0.17-1	15.0
32	1.0	0.14-1	10.0
32*	0.05	0.51-1	31.0
32*	0.02	0.36-1	77.0
64	0.4	0.74-2	130.0
64	1.0	0.98-2	88.0
64*	0.0125	0.10-7	400.0

*Explicit Second-Order Adams-Bashforth Scheme

6. Summary and Conclusions

The present investigation attempts to construct a pseudospectral scheme that is highly accurate and competitive in computational efficiency with existing finite difference or finite volume methods. Instead of examining simple model problems, we have examined realistic flows around a two-dimensional airfoil. The exterior of an airfoil is mapped to the interior of a circle by a conformal mapping. We have attempted to address several questions in applying the pseudospectral method to transonic flows with shock waves. First, a hybrid scheme based on a combined spectral-finite difference method is attempted. Various means of filtering Gibb's error are examined for their effects on numerical stability. Then, we attempt to construct a full spectral scheme using spectral discretization in both spatial dimensions. Finally, we have studied the convergence and stability of an iterative pseudospectral scheme, which could circumvent some of the problems in the construction of a full spectral scheme.

The following conclusions are made based on the results of our study:

- (1) A hybrid scheme using spectral decomposition in the direction along the airfoil surface and a finite difference scheme in the other direction is capable of resolving shock waves in one grid.
- (2) Several filters have been studied. A low-pass filter in the spectral space is not able to stabilize the computation without seriously affecting the shock resolution. An algebraic filter that averages the flow variables around a grid point is capable of stabilizing the computations and maintaining the sharpness of the shock wave.
- (3) The filter being used is stronger than the nonlinear artificial viscosity expression given by Jameson et al. (1981) except near the shock wave. Hence, the solution in the area away from the shock wave is contaminated. The drag count is substantially higher than that in a finite volume calculation. However, because of its ability in resolving a shock wave, a hybrid scheme calculation with a coarse grid can provide useful information.

- (4) The time step for an explicit hybrid scheme is smaller than that for a finite volume calculation, and it takes a substantially larger number of time steps to achieve a steady-state solution. An implicit scheme or a multigrid technique may be required to reduce the computational costs of spectral calculations.
- (5) The residue of the scheme constructed in the present investigation does not decrease with time. The number of supersonic points in the flow field is taken as an indicator of convergence. Attempts to find another form of error norm have not been successful.
- (6) An explicit full spectral scheme with a Chebyshev polynomial expansion requires excessive computing time and is not competitive with a finite volume calculation using a dense grid. A polynomial subtraction Fourier method also does not show much promise as a superior method to the finite volume method.
- (7) A Richardson iterative spectral implicit scheme has been analyzed for a simple wave equation. The analyses and the accompanying numerical experiments show that there exists an optimum convergence rate for the iteration. In order for the computations to be stable for a finite iteration scheme, a certain minimum number of iterations is required for each time step. As a result, the Fourier implicit iterative scheme does not offer any savings in computational cost for a steady-state problem. Using a Chebyshev method, savings by a factor of N in operation count can be achieved by using an iterative implicit method rather than an explicit one.

Acknowledgement

Discussions with Professors Antony Jameson and Steven Orszag of Princeton University as well as Dr. Ralph Metcalfe of Flow Industries have been very helpful. The first author would also like to express his appreciation for the constant encouragement from Mr. Morton Cooper of Flow Industries.

References

- Anderson, W. K., Thomas, J. L., and VanLeer, B. (1985) "A Comparison of Finite Volume Flux Vector Splittings for the Euler Equations," AIAA Paper No. 85-0122.
- Benjamin, T. B., Bona, J. L., and Mahony, J. J. (1972) "Model Equations for Long Waves in Non-linear Dispersive Systems," Phil. Trans. Roy. Soc. London (Ser. A.), Vol. 272, pp. 47-78.
- Gottlieb, D., and Orszag, S. A. (1977) "Numerical Analysis of Spectral Methods: Theory and Applications," CBMS-NSF Regional Conference Series in Applied Mathematics, SIAM.
- Gottlieb, D., and Turkel, E. (1980) "On Time Discretization for Spectral Methods," Studies in Applied Mathematics, Vol. 63, pp. 67-86.
- Gottlieb, D., Lustman, L., and Orszag, S. A. (1981) "Spectral Calculations of One-Dimensional Inviscid Compressible Flows," SIAM Journal of Scientific and Statistical Computation, Vol. 2, September, pp. 296-310.
- Gottlieb, D., Lustman, L., and Streett, C. (1984) "SPECTRAL Methods for Two-Dimensional Shocks," in SPECTRAL Methods for Partial Differential Equations, edited by Voight et al., SIAM.
- Hussaini, M. Y., Kopriva, D. A., Salas, M. D., and Zang, T. A., (1985a) "Spectral Methods for the Euler Equations: Part I. Fourier Methods and Shock Capturing," AIAA Journal, Vol. 23, No. 1, January, pp. 64-70.
- Hussaini, M. Y., Kopriva, D. A., Salas, M. D., and Zang, T. A., (1985b) "Spectral Methods for the Euler Equations: Part II. Chebyshev Methods and Shock Fitting," AIAA Journal, Vol. 23, No. 2, February, pp. 234-240.
- Jameson, A., and Baker, T., (1983) "Solution of the Euler Equations for Complex Configurations," AIAA Paper No. 83-1259.
- Jameson, A., Schmidt, W., and Turkel, E. (1981) "Numerical Solutions of the Euler Equations by Finite Volume Methods Using Runge-Kutta Time-Stepping Schemes," AIAA Paper No. 81-1259.
- Marcus, P. S. (1984) "Simulation of Taylor-Couette Flow: Part 1. Numerical Methods and Comparison with Experiment," J. Fluid Mech., Vol. 146, pp. 45-64.
- Orszag, S. A., and Patera, A. T. (1983) "Secondary Instability of Wall-Bound Shear Flows," J. Fluid Mech., Vol. 128, pp. 347-384.
- Riley, J. J., and Metcalfe, R. W. (1979) "Direct Numerical Simulations of the Turbulent Wake of an Axisymmetric Body," Turbulent Shear Flows II, edited by Bradbury et al., Springer-Verlag, New York.

Roache, P. (1978) "A Pseudo-Spectral FFT Technique for Non-periodic Problems," Journal of Computational Physics, Vol. 27, pp. 204-220.

Sakell, L. (1984) "Pseudospectral Solutions fo One- and Two-Dimensional Inviscid Flows with Shock Waves," AIAA Journal, Vol. 22, No. 7, pp. 929-934.

Streett, C. L. (1983) "A Spectral Method for the Solution of Transonic Potential Flow About an Arbitrary Airfoil," AIAA Paper No. 83-1949.

Taylor, T. D., Myer, R. B., and Albert, J. H. (1981) "Pseudospectral Calculations of Shockwaves, Rarefaction Waves and Contact Surfaces," Computers and Fluids, Vol. 9, December, pp. 469-473.

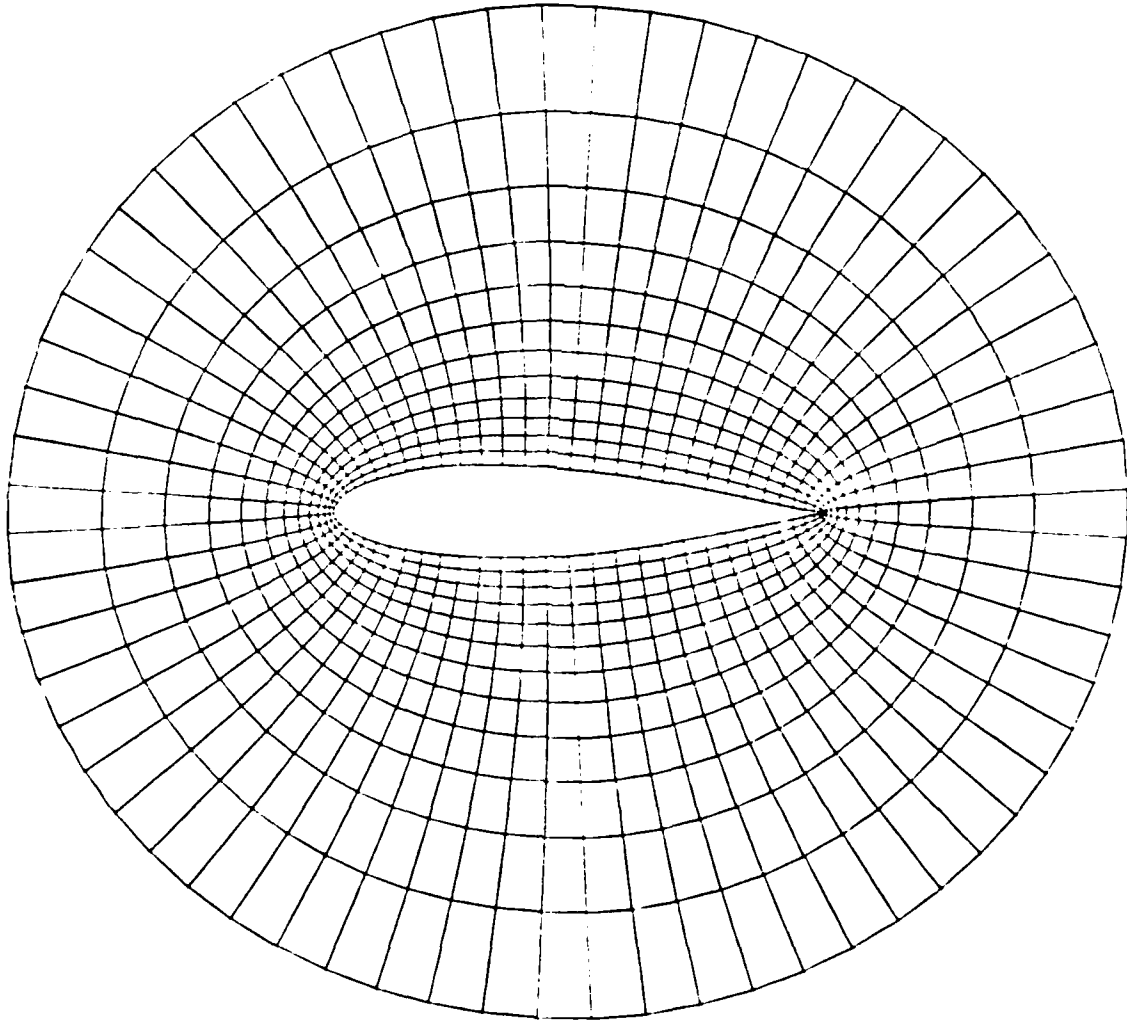


Figure 1. Computational Grid (64x16) Around a Karman-Trefftz Airfoil

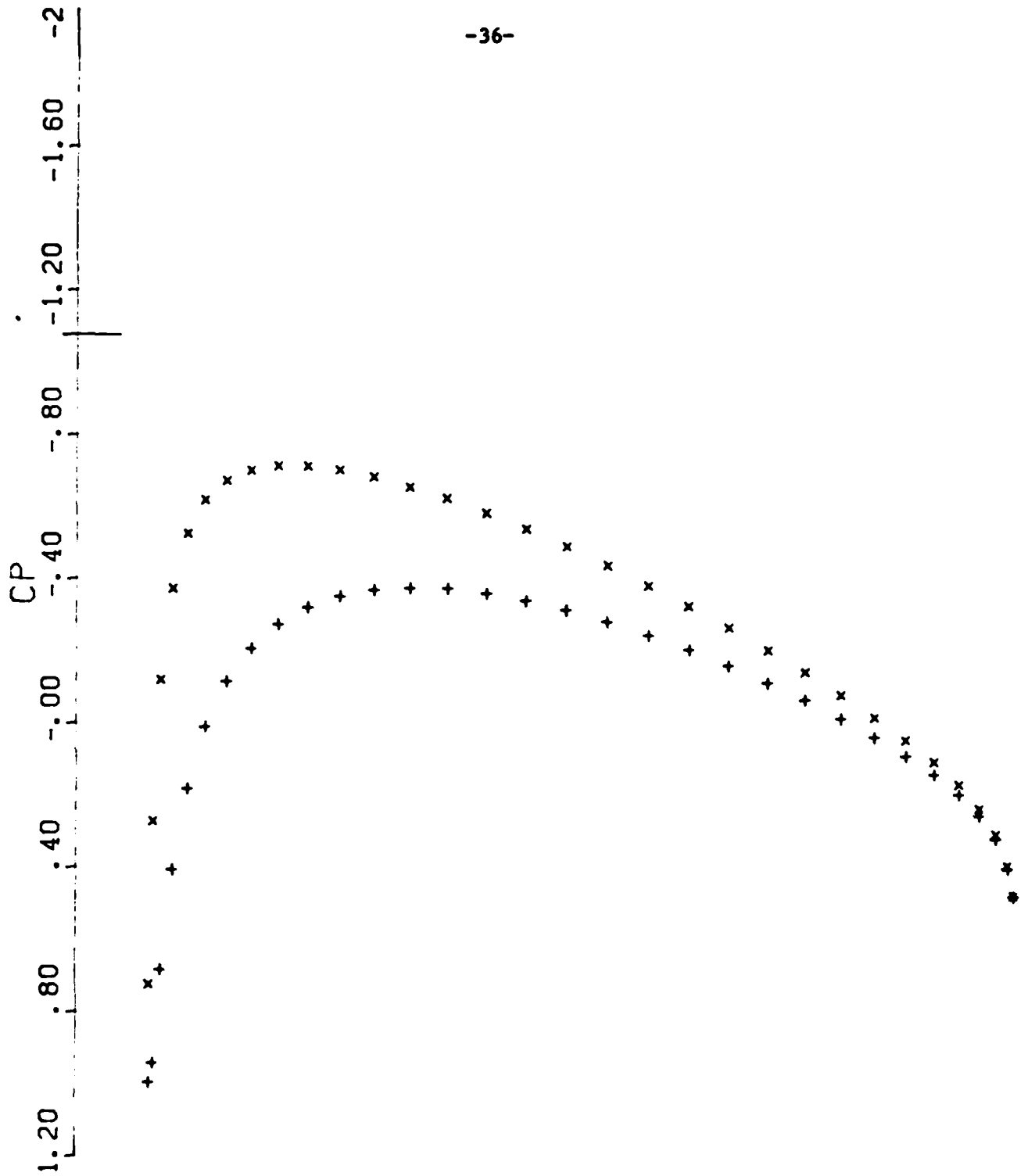


Figure 2. Hybrid Scheme--Initial Distribution of Pressure Coefficient on 64x16 Grid ($M_\infty = 0.63$; $\alpha = 2$ degrees; $C_L = 0.228$; $C_D = 0.020$)

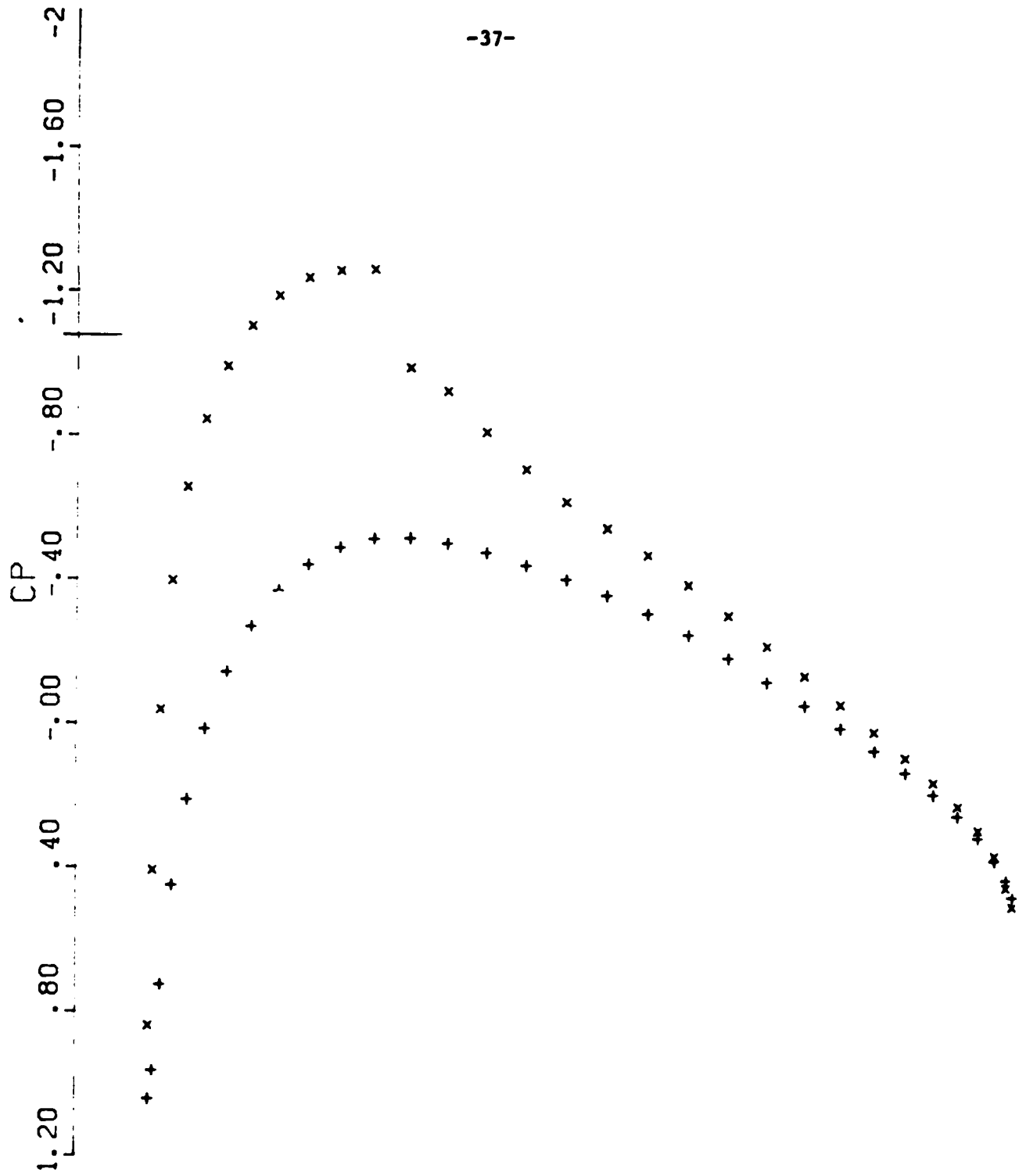


Figure 3. Hybrid Scheme--Distribution of Pressure Coefficient on 64x16 Grid After 2400 Time Steps ($M_\infty = 0.63$; $\alpha = 2$ degrees; $C_L = 0.344$; $C_D = 0.009$)

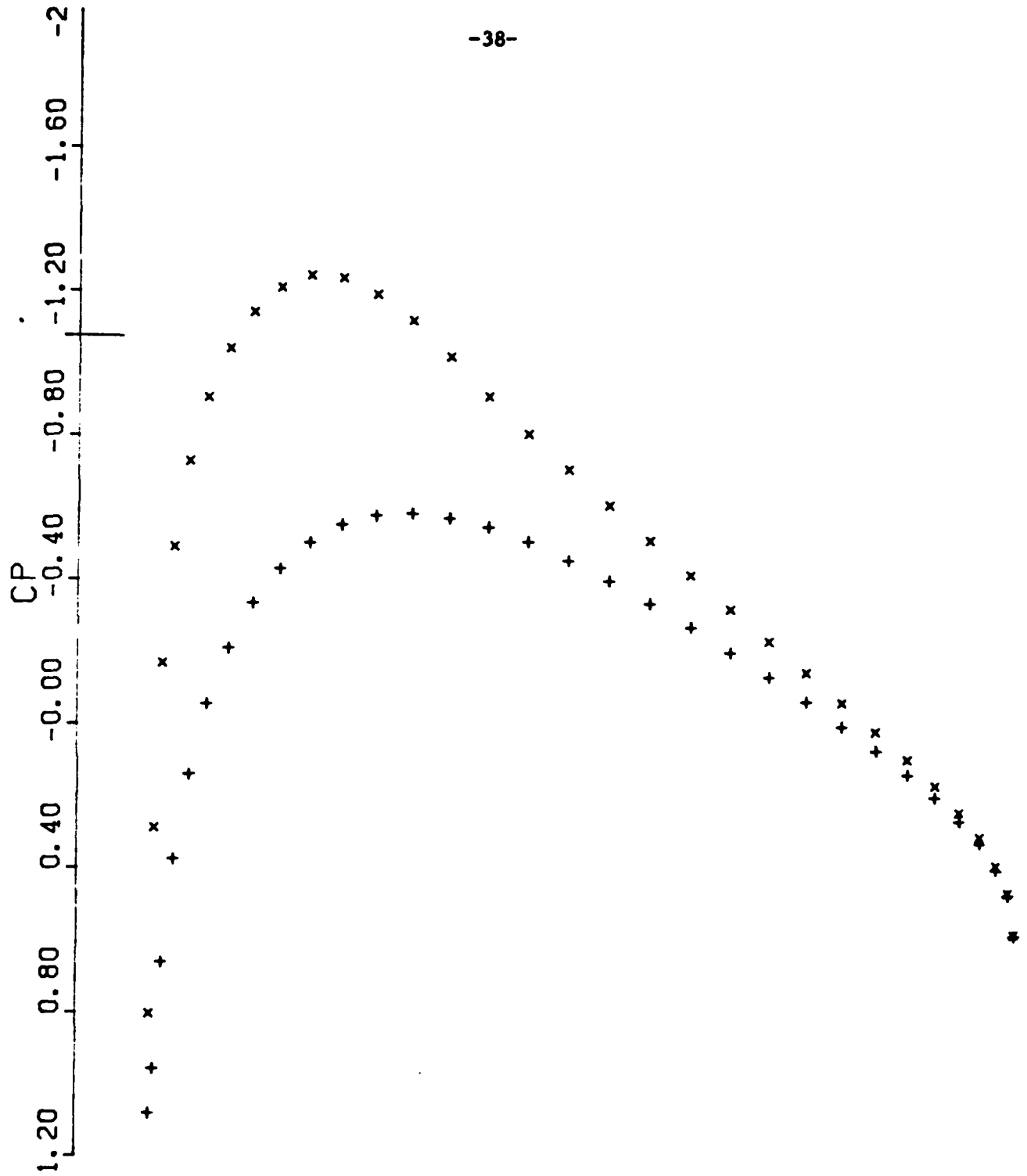


Figure 4. Finite Volume Calculation--Distribution of Pressure Coefficient on 64x16 Grid ($M_\infty = 0.63$; $\alpha = 2$ degrees; $C_L = 0.3419$; $C_D = 0.0018$; $C_M = -0.0078$)

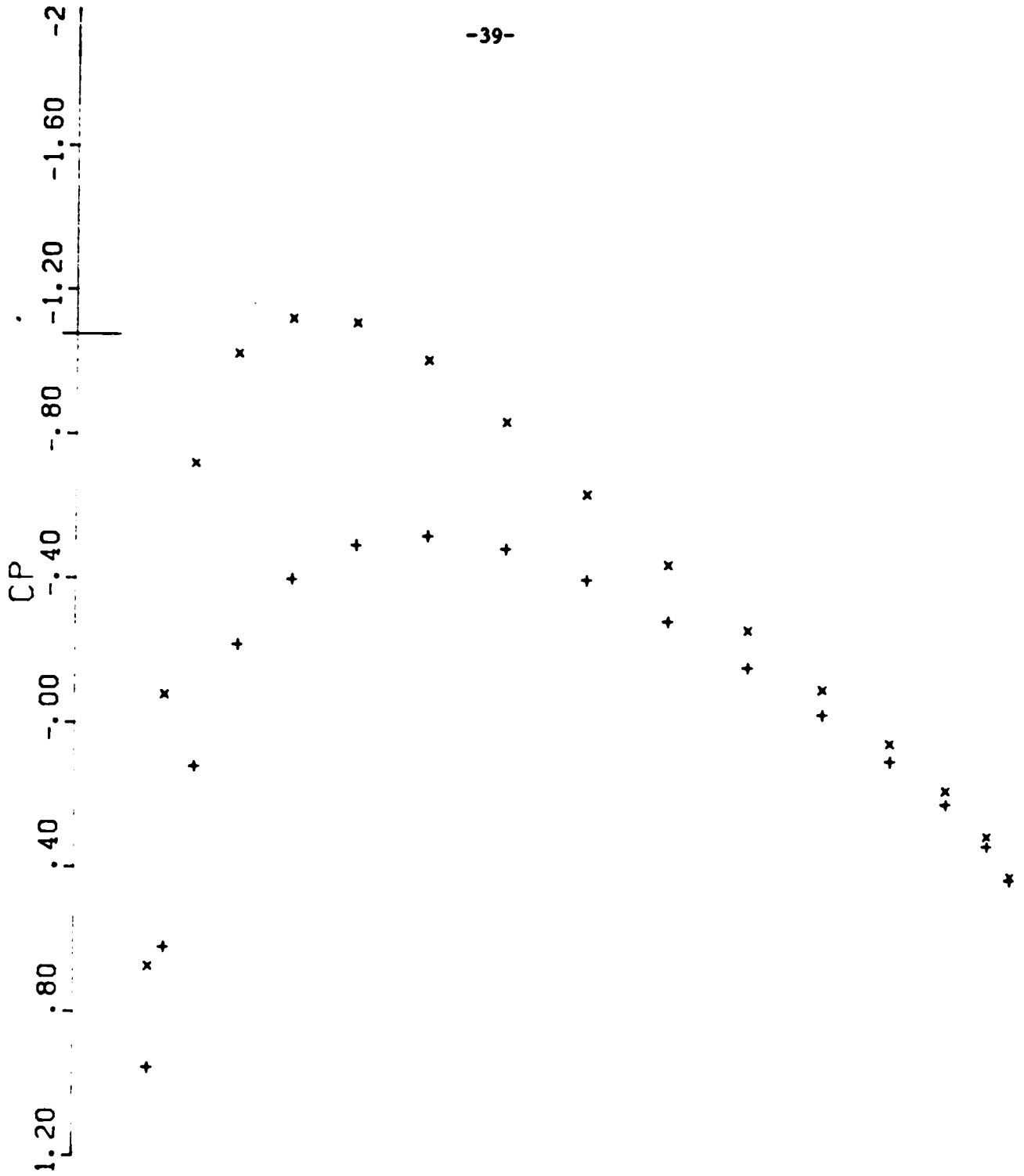


Figure 5. Hybrid Scheme--Distribution of Pressure Coefficient on 32x16 Grid ($M_\infty = 0.63$; $\alpha = 2$ degrees; $C_L = 0.333$; $C_D = 0.018$)

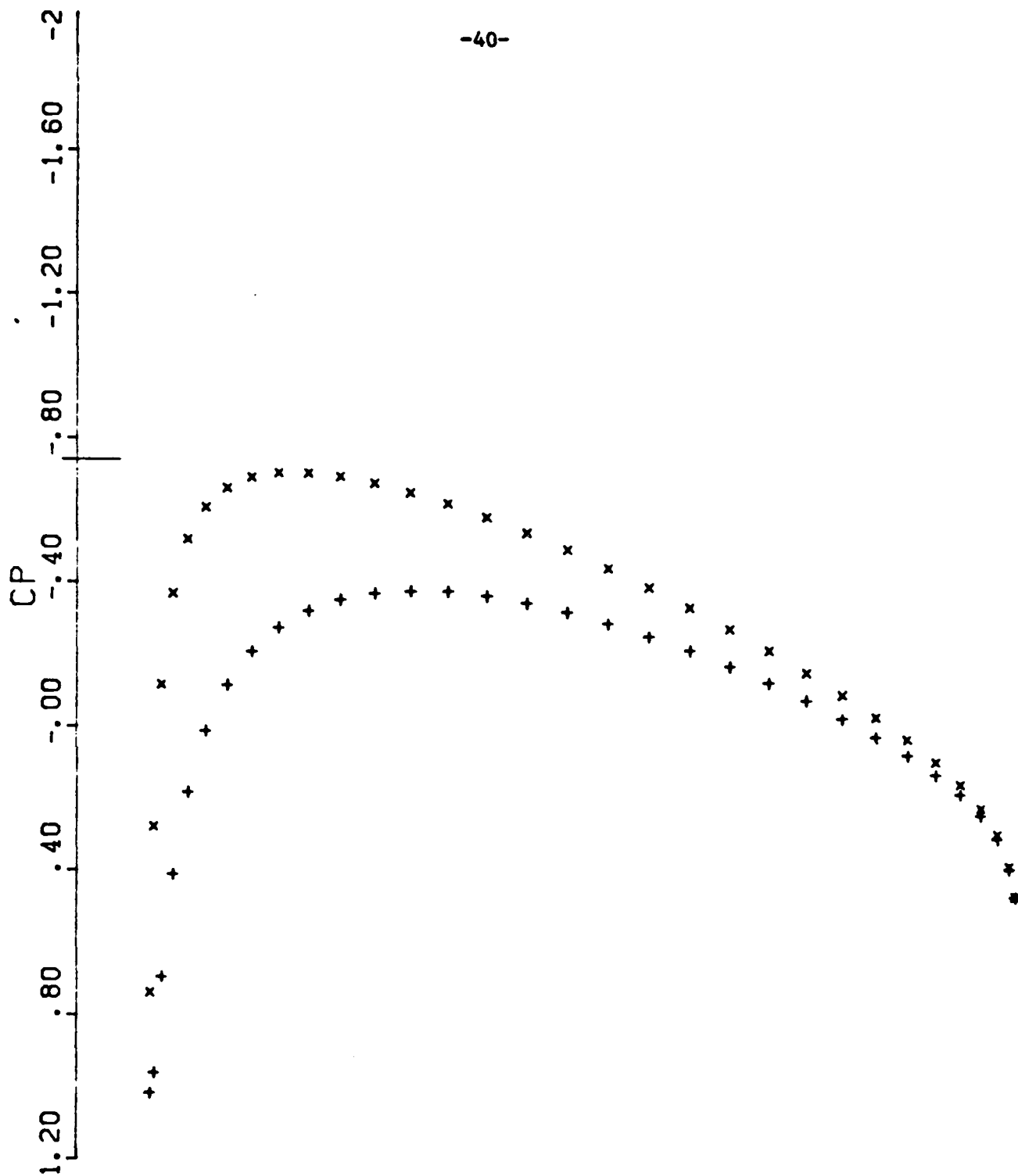


Figure 6. Hybrid Scheme--Initial Distribution of Pressure Coefficient on 64x16 Grid ($M_\infty = 0.7$; $\alpha = 2$ degrees; $C_L = 0.022$; $C_D = 0.002$)

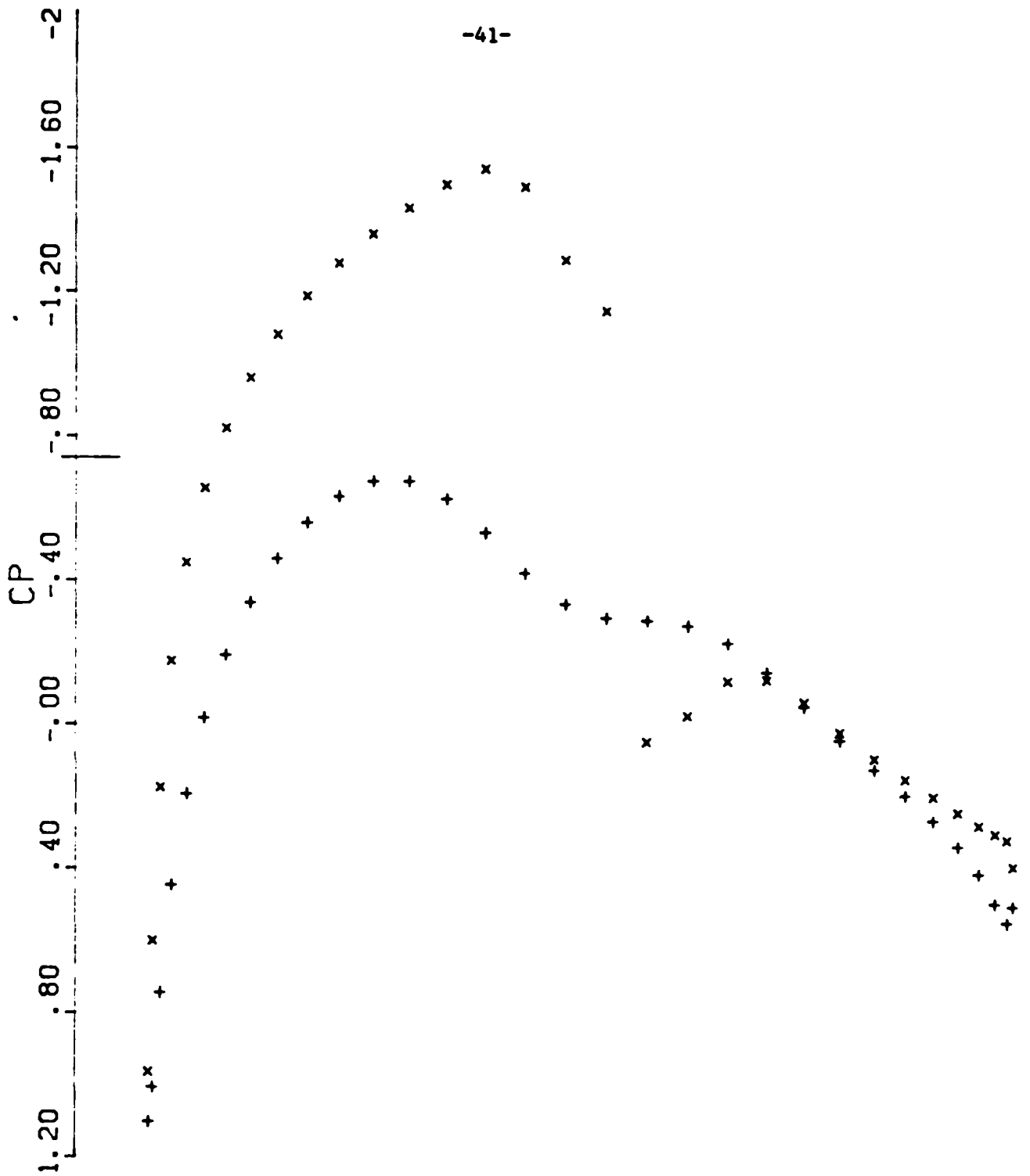


Figure 7. Hybrid Scheme--Distribution of Pressure Coefficient on 64x16 Grid After 800 Time Steps ($M_\infty = 0.7$; $\alpha = 2$ degrees; $C_L = 0.411$; $C_D = 0.019$)

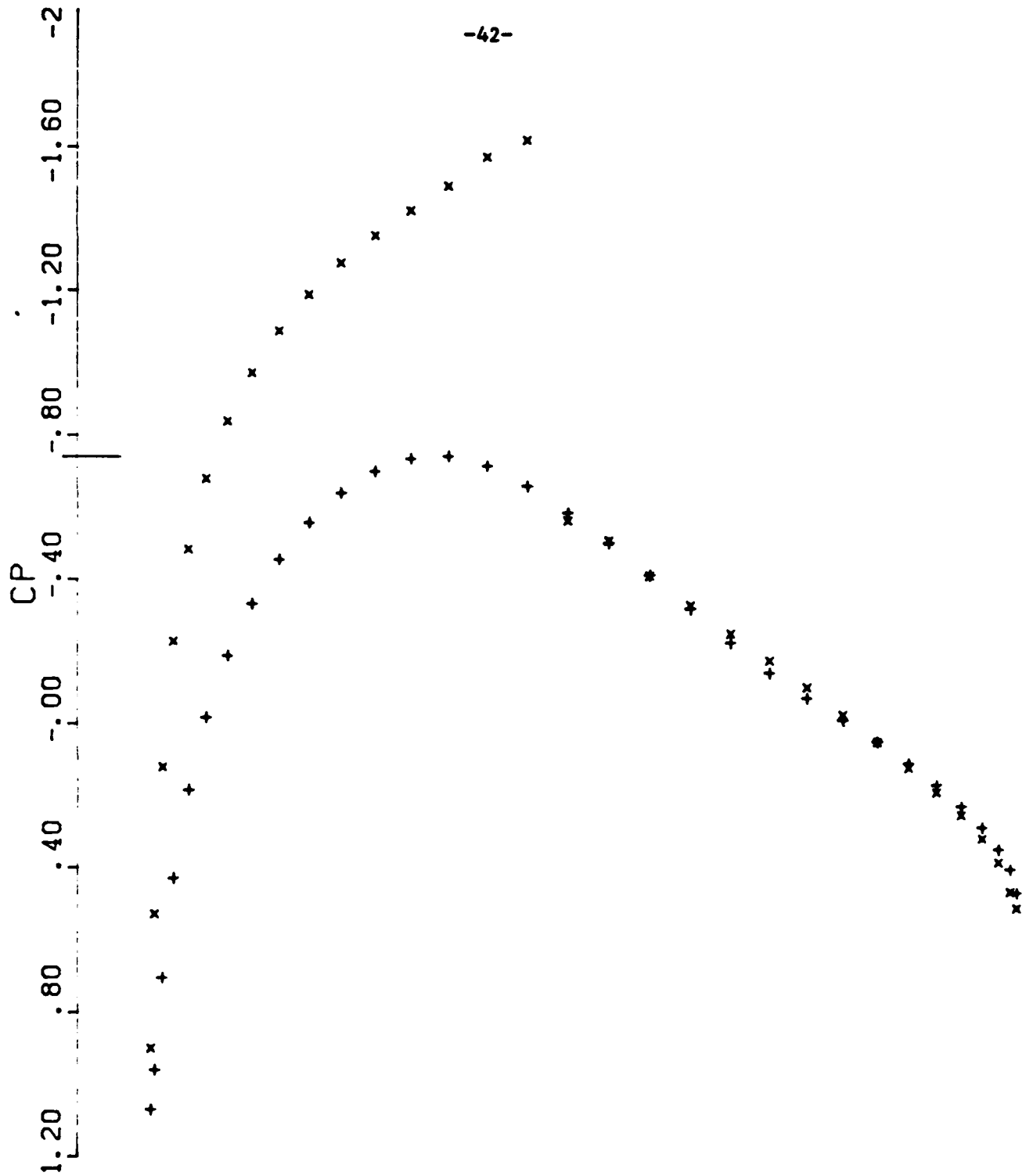


Figure 8. Hybrid Scheme--Distribution of Pressure Coefficient on 64x16 Grid After 2400 Time Steps ($M_\infty = 0.7$; $\alpha = 2$ degrees; $C_L = 0.323$; $C_D = 0.021$)

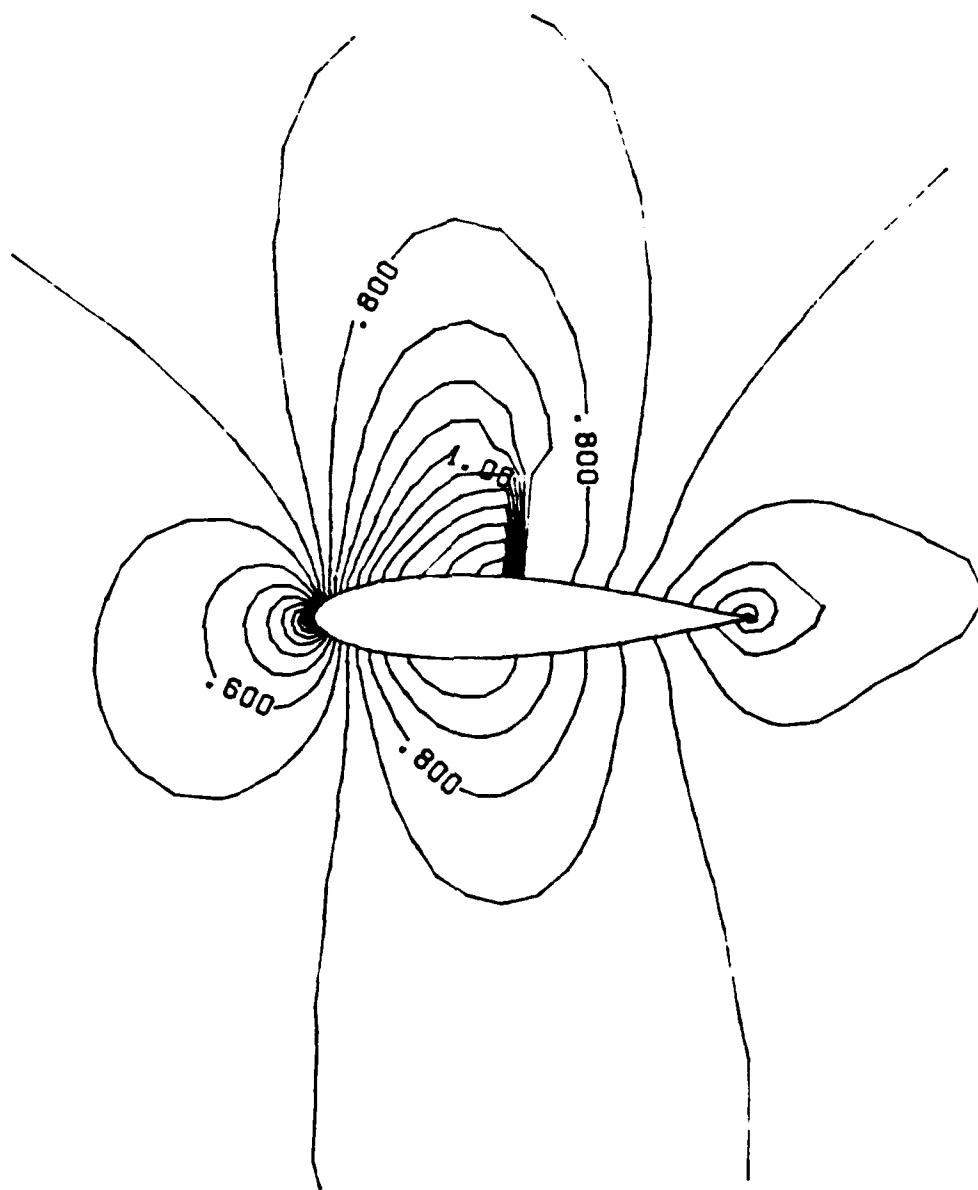


Figure 9. Hybrid Scheme--Isomach Lines in Flow Field on 64x17 Grid
($M_\infty = 0.7$; $\alpha = 2$ degrees)

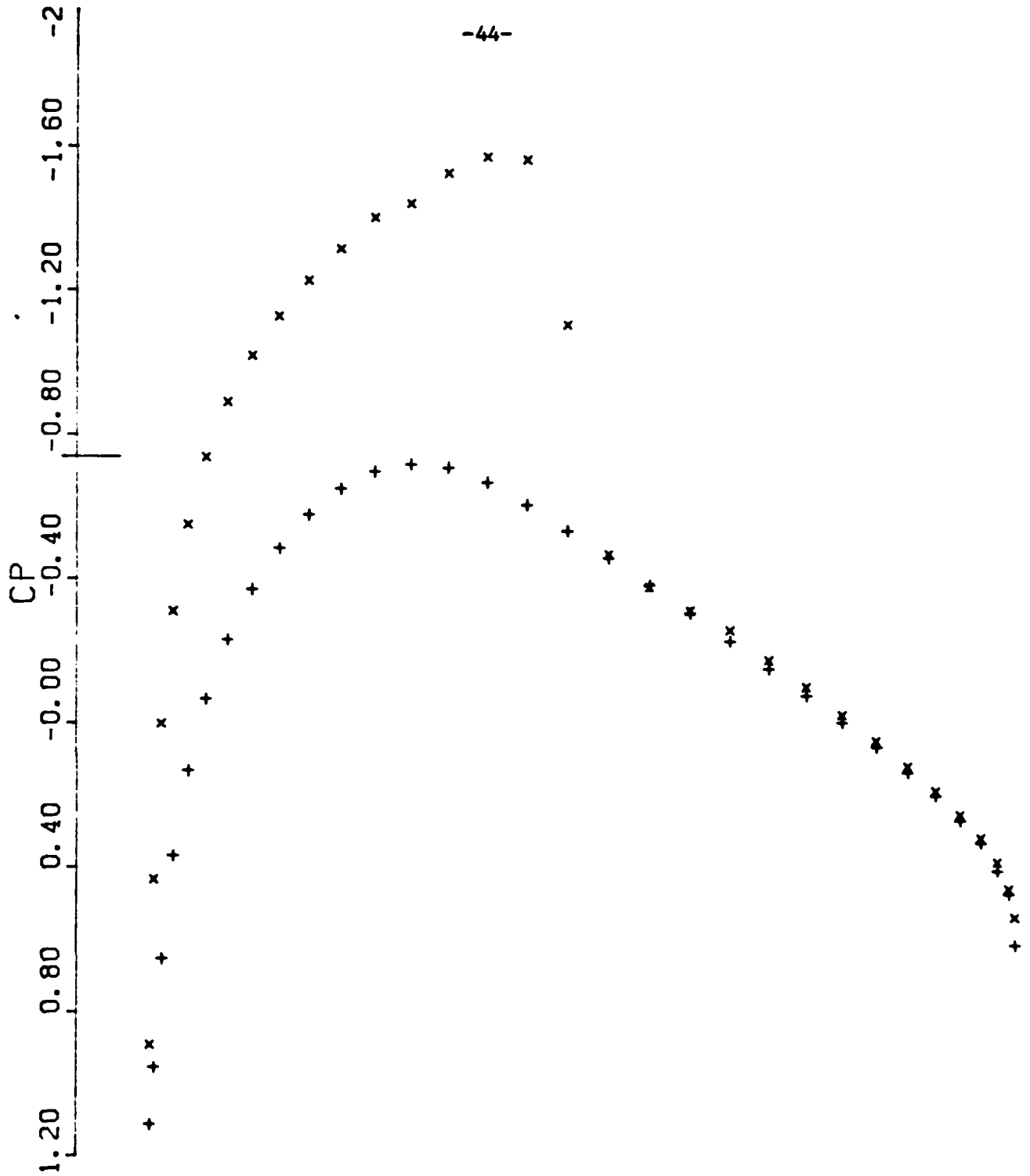


Figure 10. Finite Volume Calculation--Distribution of Pressure Coefficient on 64x16 Grid ($M_\infty = 0.7$; $\alpha = 2$ degrees; $C_L = 0.3699$; $C_D = 0.0131$; $C_M = -0.0118$)

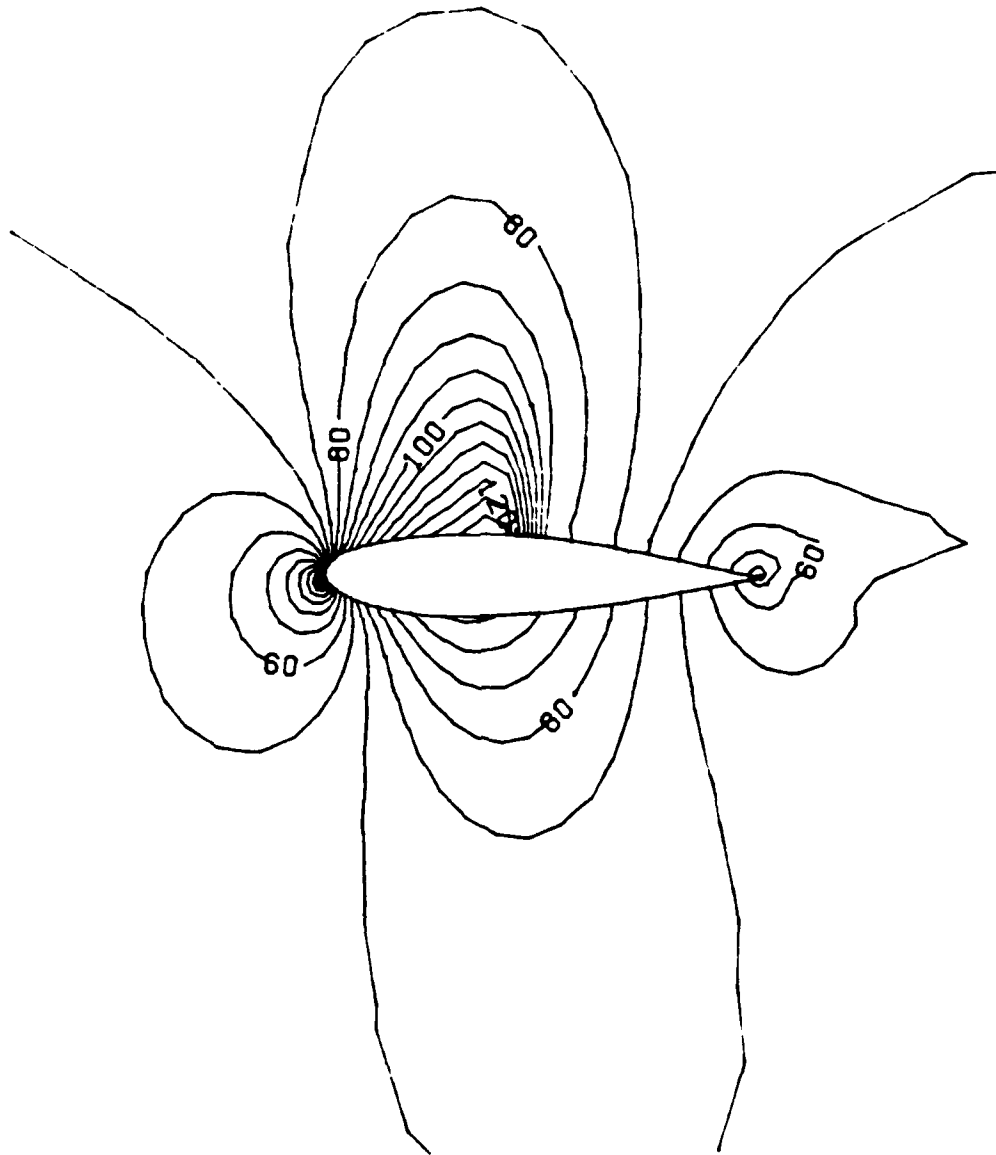


Figure 11. Finite Volume Calculation--Isomach Lines in Flow Field on 64x16 Grid ($M_\infty = 0.7$; $\alpha = 2$ degrees)

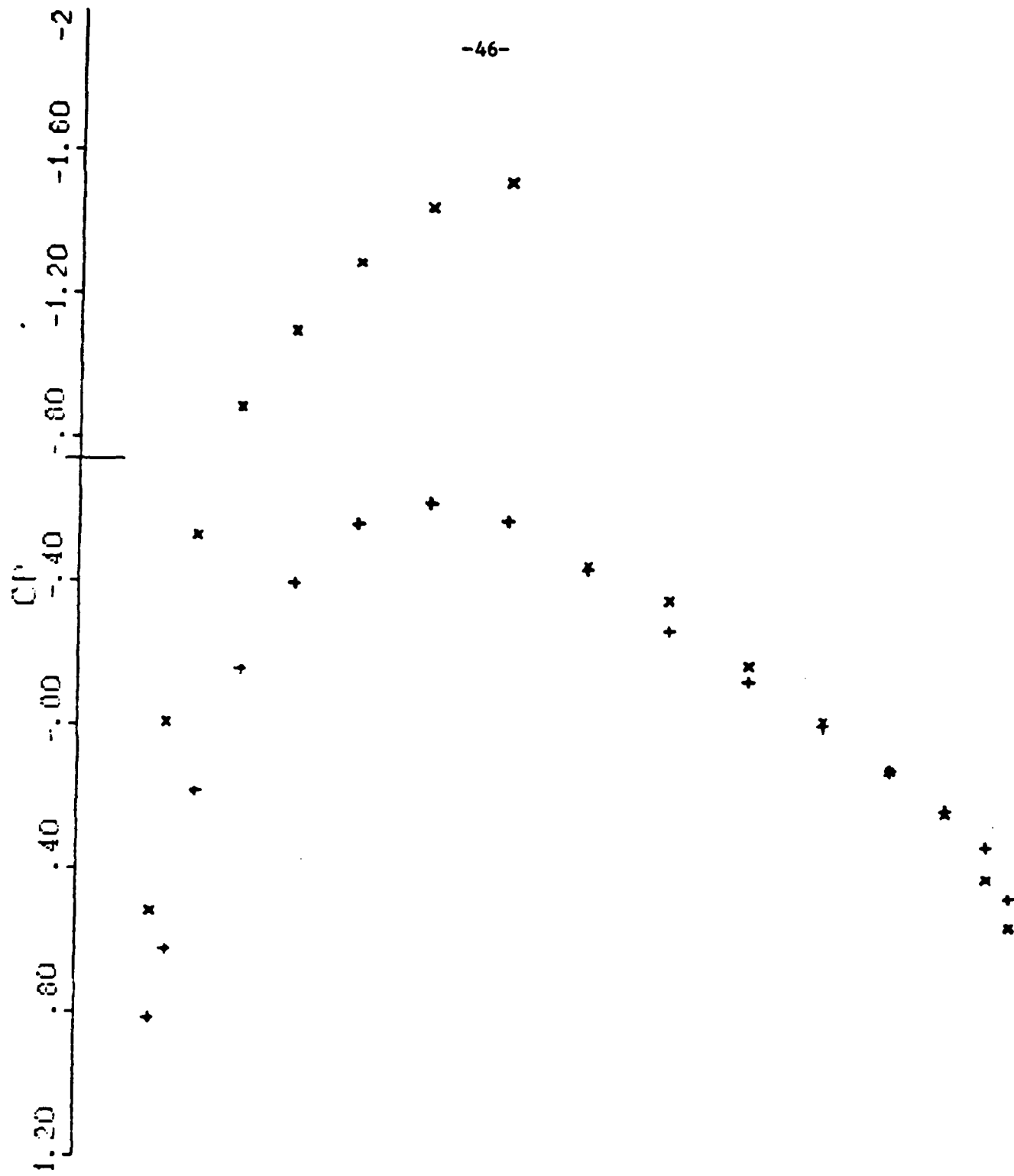


Figure 12. Hybrid Scheme--Distribution of Pressure Coefficient on 32x16 Grid ($M_\infty = 0.7$; $\alpha = 2$ degrees; $C_L = 0.362$; $C_D = 0.016$)

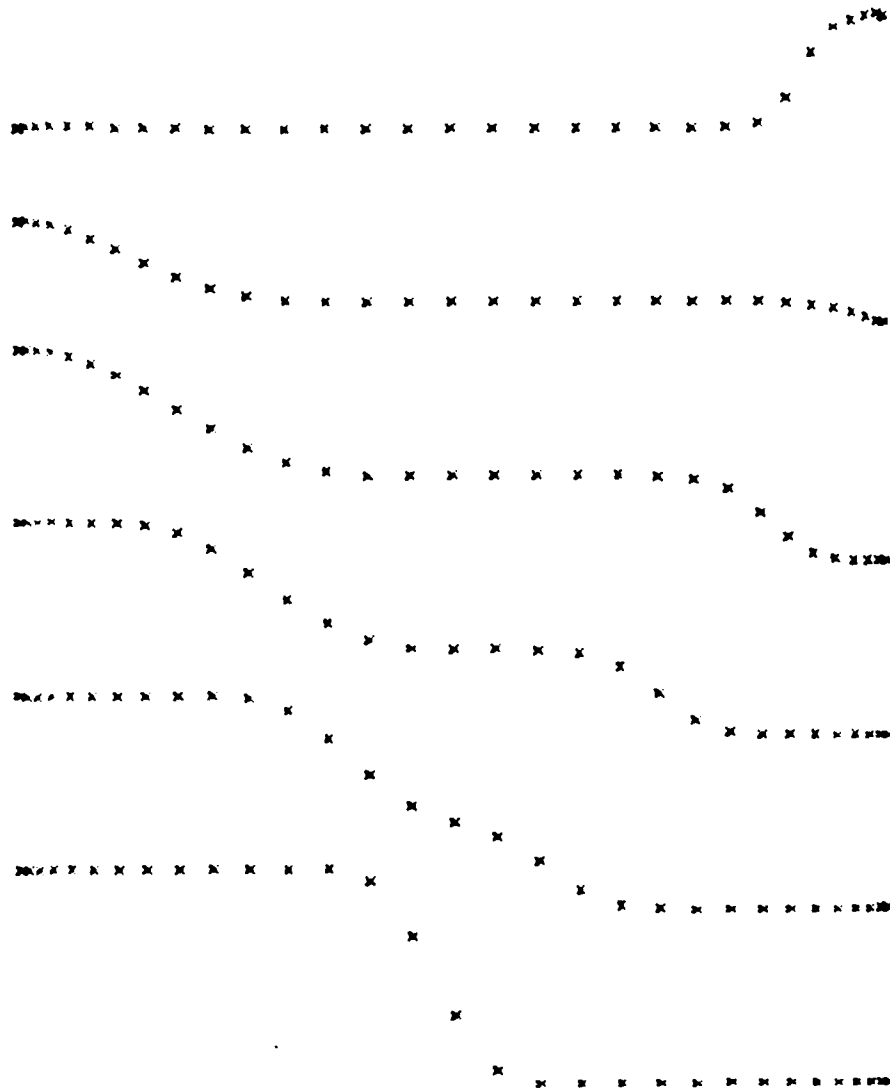


Figure 13. Chebyshev Method--Pressure Waves for One-Dimensional Problem Using 33 Grid Points

END

11-86

DT/C